Biomass Conversion to Hydrogen Using Supercritical Water

A Thesis Submitted

to the College of Graduate Studies and Research

in Partial Fulfillment of the Requirements

for the Degree of Master of Science

In the Department of Chemical and Biological Engineering

University of Saskatchewan

By

Ning Ding

Saskatoon, Saskatchewan, Canada

Permission to Use

In presenting this thesis in partial fulfillment of the requirements for a Postgraduate degree from the University of Saskatchewan, I agree that the Libraries of the University of Saskatchewan may make it freely available for inspection. I further agree that permission for copying of this thesis in any manner, in whole or in part, for scholarly purpose may be granted by the professor or professors who supervised my thesis work, or, in their absence, by the Head of the Department of Chemical and Biological Engineering or the Dean of the College of Graduate Studies and Research at the University of Saskatchewan. It is understood that any copying or publication or use of this thesis or parts thereof for financial gain shall not be allowed without my written permission. It is also understood that due recognition shall be given to me and to the University of Saskatchewan in any scholarly use which may be made of any material in my thesis.

Requests for permission to copy or to make other use of material in this thesis in whole or part should be addressed to:

Head of the Department of Chemical and Biological Engineering

57 Campus Drive

University of Saskatchewan

Saskatoon, Saskatchewan, Canada

S7N 5A9

Acknowledgements

I would first like to thank my supervisors, Dr. Ajay. K. Dalai and Dr. Janusz A. Kozinski, for their mentorship, valued guidance and critical supervision throughout my master study.

Many thanks also to my advisory committee members, Dr. Jafar Soltan and Dr. Catherine Niu, for their contributions to my graduate studies and the time taken to review and critique my written materials.

I would like to thank Dr. Ramin Azargohar and Dr. Morgan Thomas for their guidance, contribution and encouragement. I would also like to thank Mr. Richard Blondin, Ms. Heli Eunike and Mr. Rlee Prokopishyn for their assistance in carrying out the laboratory work that contributed to my project.

I would like to express my gratitude to all members of the catalysis and chemical reaction engineering laboratories, who were always supportive during my graduate study at in the University of Saskatchewan.

I should like to thank all the faculty in Department of Chemical and Biological Engineering for their support.

Last but not least, I would like to thank my beloved parents and all my friends for their continued support.

Dedicated to my loving parents.

Abstract

In this work, SCWG of glucose, cellulose and pinewood was studied at different operating conditions with and without catalyst. Three parameters studied included temperature (400, 470, 500 and 550^{o}C), water to biomass weight ratio (3:1 and 7:1) and catalyst (Ni/MgO, Ni/activated carbon, Ni/Al_2O_3, Ni/CeO_2/Al_2O_3, dolomite, NaOH, KOH, activated carbon and olivine), which were varied for gasification of glucose, cellulose and pinewood. By comparing the results from model compound (glucose and cellulose) with that from real biomass (pinewood), the mechanism of how the individual compounds are gasified was explored.

For catalytic runs with glucose, NaOH had the best activity for improving H_2 formation. H_2 yield increased by 135% using NaOH compared to that for run without catalyst at 500^{o}C with a water to biomass weight ratio of 3:1. At the same operating conditions, the presence of Ni/activated carbon (Ni/AC) contributed to an 81% increase in H_2 yield, followed by 62% with Ni/MgO, 60% with Ni/CeO_2/Al_2O_3 and 52% with Ni/Al_2O_3.

For catalytic runs with cellulose, the H_2 yield increased by 194% with KOH compared to that for run without catalyst at 400^{o}C with a water to biomass ratio of 3:1. At the same operating conditions, the presence of Ni/CeO_2/Al_2O_3 contributed to a 31% increase in H_2 yield followed by a 28% increase with dolomite.

When the water to biomass ratio was increased from 3:1 to 7:1, H_2 yield from glucose gasification was increased by 40% and 33% at 400 and 500^{o}C, respectively, and the H_2 yield of cellulose gasification was increased by 44%, 11% and 22% at 400, 470 and 550^{o}C, respectively. The higher heating value of the oil products derived from SCWG of both glucose and cellulose incresed in the presence of catalysts.

As real biomass, pinewood was gasified in supercritical water at the suitable operation conditions (550^{o}C with water to biomass ratio of 7:1) obtained from previous experiments, using three kinds of catalyst: Ni/CeO_2/Al_2O_3, dolomite and KOH. At the same operating conditions, the gasification of pinewood had smaller yields of H_2 (20 to 41%) compared with that from cellulose.

The effect of the catalyst on H_2 production from SCW in the absence of biomass was studied. The results showed that a trace amount of H_2 was formed with Ni based catalyst/dolomite only while some CO_2 was formed with Ni/AC.

Most of the runs presented in this report were repeated once, some of the runs had been triplicated, and the deviation of all results was in the range of ±5%.

Keywords

Gasification, Biomass, Catalyst, Supercritical water (SCW), Hydrogen, Supercritical water gasification (SCWG)

rTable of Contents

List of Tables

List of Figures

List of Abbreviations

AC: Activated carbon

CE: Carbon efficiency

CSCWG: Catalytic supercritical water gasification

FTIR: Fourier transform infrared

GHGs: Greenhouse gases

GPC: Gel permeation spectroscopy

HHV: Higher heating value

LHV: Lower heating value

SCWG: Supercritical water gasification

SCW: Supercritical water

XRD: X-ray diffraction

1. Introduction

Energy shortage and environmental pollution are two main challenges we have to deal with in the future. With the increasing consumption of fossil fuels, much research was focused on renewable energies such as solar and biomass in recent years (Guo *et al*. 2010). Renewable energy, particularly biomass, is therefore becoming increasingly important for sustainable development. Bio-energy (energy derived from biomass) is an immense source of renewable energy which will not run out. Biomass contributes approximately 12% of the global primary energy supply and about 40–50% in many developing countries (Yu *et al*. 2008). The analysis carried out by the United National Conference on Environment and Development shows that biomass will potentially supply about half of the world primary energy consumption by the year 2050 (Aymonier *et al*., 2006). In the meantime, biomass is an environmentally friendly energy resource; it can capture the greenhouse effect gases released into the atmosphere by its combustion through photosynthesis (Letellier *et al*. 2010). Thus, there is no net increase in CO_2 concentration. The contents of sulphur, nitrogen and metals are also very low, therefore there are fewer SO_x, NO_x emissions and other toxins released into the atmosphere during biomass combustion. Therefore, biomass is recognized as an important part of any strategy to address the environmental issues related to fossil fuel usage (Yu *et al*. 2008).

1.1 Background of the project

Lignocellulose biomass can be used to produce fermentable sugars and then ethanol, which has great potential to replace petroleum fuel. However, lignocellulose is difficult to convert to fermentable sugars. The conventional method needs several steps: drying the biomass, physical and/or chemical pretreatment, enzymatic hydrolysis or acid hydrolysis, fermentation of C5 and C6 sugars by microorganisms and distillation. This complicated process is energy-intensive. Recently, therefore subcritical and supercritical water have been found to be efficient ways of producing fermentable hexoses from lignocellulosic materials (Schacht *et al*. 2008). Compared with conventional methods for producing fermentable sugars, the use of sub/supercritical water has a significantly higher reaction rate and there is no need of using catalysts or harmful acid solvents.

Furthermore, biomass can be converted to syngas in SCW at relatively high temperatures. The yield and composition of the gas products and other products depend on the gasification conditions and the composition of the biomass. The gas products are mainly of hydrogen, carbon dioxide and methane and with small amount of carbon monoxide, methane, ethane, ethene, propane and propene (Yanik *et al*., 2007). These gases can be used for different applications according to their composition. Most of the carbon monoxide produced is expected to come from water soluble organic compounds that were the first products from lignocellulosic material gasification, and it is consumed through the water–gas shift reaction and the methanation reaction (Yanik *et al*., 2007). Several studies have shown that the use of catalysts, such as ZrO_2 and RuO_2, during biomass treatment in SCW can produce hydrogen and methane rich gases while suppressing char formation (Watanabe *et al*., 2002). Hydrogen is a renewable and green alternative energy source and it has attracted extensive attention worldwide. Hydrogen can be used for machinery with zero emission as well as for high thermal efficiency hydrogen fuel cells (Guo *et al*., 2010). Nowadays, large amounts of hydrogen gas are used in the petrochemical and chemical industries and there is growing interest in the use of hydrogen as fuel (Yanik *et al*., 2007). However, hydrogen is a gas that is not directly available in nature; it must be produced from various substances containing H_2.

In classical processes for biomass gasification (downdraft gasifier, entrained flow gasifier), the biomass needs to be dry enough to ensure a high conversion efficiency. However, when treating biomass in subcritical or supercritical water, there is no need to evaporate the water prior to the gasification (Letellier *et al*., 2010). Moreover, subcritical or supercritical water has the unique characteristic of dissolving materials not normally soluble in either the liquid or the vapor phase.

1.2 Knowledge Gap

Much research has been conducted on sub- and supercritical water technologies for biomass conversion, but the majority of them were focused on biomass model compounds, mainly cellulose and lignin. Real biomass was not widely studied.

Continuous research is necessary to explore the effect of the catalyst on H_2 production from water in the absence of biomass. Most research does not take into consideration reactions between H_2O and the catalysts

The effect of different Ni-based catalysts has rarely been studied at the same operating conditions to compare their catalytic activities.

1.3 Objective of the Work

This research aims at finding suitable conditions including temperature and water to biomass ratio for supercritical water gasification of biomass within the range of parameters studied.

The objective is also to study SCWG of glucose, cellulose and pinewood to develop a better understanding regarding role of each individual component in SCWG of biomass.

The objective is to study the effect of catalysts on H_2 production from water in the absence of biomass

Ni-based catalysts and alkali catalysts, as well as dolomite and olivine, were studied to compare their catalytic activities for SCWG.

1.4 Thesis Organization

The remainder of the thesis is organized as follows: Chapter 2 discusses the reaction chemistry of biomass gasification, the parameters that influence the gasification process and the effect of different kinds of catalysts. Chapter 3 introduces the preparation of catalyst, the experimental procedures and the characterization methods used in this research. Chapter 4 presents the experimental results, provides the respective discussion and leads to conclusions. Chapter 5 lists the research conclusions and includes some recommendations for future research.

2. Literature review

2.1 Starting Material: Biomass (Lignocellulose)

Biomass can be classified into four categories: agriculture, forest, municipal solid waste and others, such as fast growing plants, short-rotation crops, herbage plants and ocean biomass. Biomass typically consists of 25% lignin and 75% carbohydrate (i.e. cellulose and hemicellulose). Cellulose, hemicellulose and lignin are the building blocks of lignocellulose biomass. Therefore, many researchers have utilized model compounds, such as cellulose, glucose, xylan and phenol, to simulate the behavior of real biomass. Lignocellulose forms a complex crystalline structure held together by covalent bonding, intermolecular bridges and van-der-Waals force and which is resistant to attack by enzymes and is insoluble in water (Schacht *et al*. 2008). Meanwhile, biomass contains other minor substances, including minerals and organic molecules such as tannins, terpenes, waxes, fatty acids and proteins (Serani *et al*., 2010).

Cellulose $(C_6H_{10}O_5)_n$ is a polysaccharide consisting of a linear chain of several hundred to over ten thousand $\beta(1\rightarrow4)$ linked D-glucose units (Gardner and Blackwel, 1974). Cellulose can be considered as a condensation polymer of glucose, similar to starch, but the links between the glucose monomers are slightly different. Because of its low-surface-area crystalline form held together by hydrogen bonds, cellulose is insoluble in water. The highly ordered crystallites of cellulose can be broken up by strong acids and alkalis, thus cellulose can be swelled, dispersed and even dissolved (Yu *et al*., 2008).

Hemicellulose has a random, amorphous structure with little strength. It can be easily hydrolyzed by dilute acid or base as well as by myriad hemicellulose enzymes (Peterson et al., 2008). Hemicellulose contains many different sugar monomers. In contrast, cellulose contains only anhydrous glucose. In addition, hemicellulose is a branched polymer, whereas cellulose is unbranched.

Lignin is a complex chemical compound most commonly derived from wood, and an integral part of the secondary cell walls of plants and some algae. As a biopolymer, lignin is unusual because of its heterogeneity and lack of a defined primary structure. Its most commonly noted function is support through strengthening of wood (xylem cells) in trees. Lignin is often

associated with cellulose and hemicellulose materials making up lignocellulose compounds, which must be broken down to make the cellulose or hemicellulose accessible to hydrolysis (Peterson et al., 2008). Lignin has an amorphous structure, which leads to a large number of interlinkages between individual units (Yu *et al*., 2008). Unlike the acetal functions found in cellulose and hemicelluloses, ether bonds predominate between lignin units

Biomass may also contain a wide range of organic extractives, which can be separated using polar or nonpolar solvents. The extractives include fats, waxes, alkaloids, proteins, phenolics, simple sugars, pectins, mucilages, gums, resins, terpenes, starches, glycosides, saponins and essential oils (Yu *et al*., 2008). Extractives function as intermediates in metabolism, energy reserves, and protective agents against microbial and insect attack. As a result of nutrient uptake during the growth of biomass, there are also some inorganic extractives in biomass, such as potassium, sodium, calcium, etc. (Yu *et al*., 2008).

2.2 Production of Fuel Gas from Gasification: Conventional Methods

Generally, conventional gasification is carried out at 700-1000^{o}C, atmospheric pressures without catalyst. The gas product has different applications depending on its composition. The earliest practical production of synthetic gas (syngas) is reported to have taken place in 1792, when a Scottish engineer pyrolyzed coal and used the product, coal gas, to light his home. In the latter half of the 19th century, coal gasification became a commercial reality through the use of cyclic gas generators, also known as air-blown gasifiers. As feedstock proceeds through a gasification reactor or gasifier, the following processes may occur (Higman and Burgt, 2003).

1. Drying

As the feedstock is heated and its temperature increases, water is the first constituent to evolve.

$$Moist\ feedstock \rightarrow Dry\ feedstock + H_2O \quad (2.1)$$

2. Devolatilization

As the temperature of the dry feedstock increases, pyrolysis takes place and the feedstock is converted to char.

$$Dry\ feedstock \rightarrow Char + Volatiles \quad (2.2)$$

Depending on the origin of the feedstock, the volatiles may include H_2O, H_2, N_2, O_2, CO_2, CO, CH_4, H_2S, NH_3, C_2H_6 and very low levels of unsaturated hydrocarbons such as acetylenes, olefins, aromatics and tars. Char is the residual solids consisting of organic and inorganic materials. After pyrolysis, the char has a higher carbon content than the dry feedstock (Higman and Burgt, 2003).

3. Gasification

Gasification is the result of chemical reactions between carbon in the char and steam, carbon dioxide and hydrogen in the gasifier vessel, as well as chemical reactions between the resulting gases (Higman and Burgt, 2003).

$$C+H_2O \rightarrow CO+H_2 \quad (2.3)$$

$$C+2H_2O \rightarrow CO_2+2H_2 \quad (2.4)$$

$$C+CO_2 \rightarrow 2CO \quad (2.5)$$

$$C+2H_2 \rightarrow CH_4 \quad (2.6)$$

$$CO+3H_2 \rightarrow CH_4+H_2O \quad (2.7)$$

$$CO+H_2O \rightarrow H_2+CO_2 \quad (2.8)$$

2.2.1 Coal gasification

The gasification of coal is essentially the conversion of coal to produce combustible gases. Primary gasification is the thermal decomposition of coal to produce syngas, as well as products such as tar, oils and phenols. A solid char product may also be produced and react with water vapor in the secondary gasification (Kroschwitz *et al*., 1991).

$$C_{char}+H_2O \rightarrow CO+H_2 \quad (2.9)$$

The gaseous product from a gasifier generally contains large amounts of carbon monoxide and hydrogen, plus lesser amounts of other gases.

2.2.2 Gasification from other fossil fuels

Thermal pyrolysis of petroleum or its fractions is an important method for producing fuel gas. In the 1940s, the hydrogasification of oil was investigated as a follow-up to work on the hydrogasification of coal (Rezaiyan and Cheremisinoff, 2005).

$$CH_{petroleum} \rightarrow CH_4 \tag{2.10}$$

As in the case of coal, synthetic natural gas can be produced from heavy oil by partially oxidizing the oil to a mixture of carbon monoxide and hydrogen (Rezaiyan and Cheremisinoff, 2005).

$$2CH_{petroleum} + O_2 \rightarrow 2CO + H_2 \tag{2.11}$$

2.2.3 Biogasification

Biogasification may be considered a clean technology because of the reduction in CO_2 emissions, the equipment has a relatively small footprint and is compact, there is a high thermal efficiency and a good degree of combustion control, and in areas where biomass sources are readily available at low prices, gasifier systems offer economic advantages over other energy generating technologies (Higman and Burgt, 2003).

Biogas can be used for a variety of applications, which include thermal energy for cooking, boiling water, steam generation and drying, in power applications such as diesel engines and for electricity generation.

Organic tars are a major concern in biomass gasification. Tar is a condensable fraction of the gas product and contains components which are largely aromatic hydrocarbons with molecular weights greater than that of benzene, and can cause plugging in pipes, filters, fuel lines, etc. In order to use biomass in commercially advanced gasification technologies, it is necessary to remove, convert or deconstruct the tar contained in the gas product (Higman and Burgt, 2003).

2.3 Supercritical water for the production of fuel gas

Most industrial processes for hydrogen production have to use reforming techniques, which require hydrocarbons, stemming from oil industry. Therefore, hydrogen produced in that way

can no longer be considered as a clean gas, especially because of its bonds with oil production, which is limited by geopolitical aspects and by carbon dioxide formation (Yanik *et al*., 2007). One of the processes is biomass gasification, which has the advantage of recovering wastes. This process can be used to synthesize not only hydrogen but also fuels and a large number of chemical compounds.

The conventional hydrogen production methods have some shortcomings: electrolysis of water has a very high production cost, water photolysis is until now just under laboratory study at present, thermal pyrolysis and reforming of organic compounds need a dehydration process for the pretreatment of wet feed and hydrogen production *via* methanation by microorganism has a slow reaction rate and low conversion efficiency (Guo *et al*., 2010).

Compared with conventional gasification methods, the supercritical water gasification (SCWG) process has high reaction efficiency and H_2 selectivity. Water is a reaction medium and there is no need to dry the biomass prior to the process. Therefore, for wet biomass containing large amounts of water up to 90%, SCWG appears to be a useful technology (Calzavara *et al*., 2005). Another advantage of gasification in SCW is the high solid conversion, i.e. low levels of char and tars. SCW has better flowability and carrying capacity, which can decrease the yield of coke, and thus prolong the service life of the catalyst. SCW treatment of biomass has a high reaction rate, and would produce gaseous products in high concentration. Furthermore, as there is no limit of interphase mass transfer resistance the reactions proceed very rapidly and completely (Kruse *et al*., 2005). SCWG is one of the hydrogen production methods with great potential.

However, SCWG reactions have some deficiencies, such as the need for high temperature and pressure. The composition of the gas product, to a large extent, depends on operating conditions. Early investigations have found that a high yield of hydrogen can be obtained only when the temperature is higher than 600^{o}C (Tang *et al.* 2005). At low temperatures (<450^{o}C), the major product is CH_4. The reactions during SCWG process are exothermic, but they cannot maintain through self-sufficiency the minimum temperature that the reactions need, so the economic efficiency has to be dealt with in the further development of SCWG (Calzavara, 2005).

Furthermore, the biogas generated from SCWG will generally contain contaminants that need to be removed. The principal contaminant classes encountered are particulates, alkali compounds,

tars, nitrogen-containing components, sulfur and low-molecular-weight hydrocarbons. The presence of tars in the product gas is highly undesirable in synthesis gas for hydrogen application. Tar formation represents a reduction in gasification efficiency since less of the biomass is converted to a fuel or synthesis gas. More importantly, tars would reduce the performance of gasification systems. Tars in the biogas can be tolerated in some systems where the gas is used as a fuel in closely coupled applications such as burners. In these situations, cooling and condensation can be avoided, and the energy content of the tars adds to the calorific value of the fuel. However, in more demanding applications, tars in the raw product gases can create handling and disposal problems. Tars condense on cold components downstream from the gasifier, resulting in plugging and fouling of pipes, tubes and other equipment. At temperatures above about 400^{o}C, tars can undergo dehydration reactions to form solid char and coke that further fouls and plugs systems. Also, tar formation presents a cleanup problem and costly disposal of a hazardous waste.

In order to reduce equipment investment and operating cost, and to reduce the needed temperature and pressure, some researchers add a suitable hydrothermal catalyst to reduce the activation energy, and thus increase the reaction rate. Consequently, catalytic supercritical water gasification (CSCWG) is becoming an important research direction.

2.4 Properties of water near or at the critical point

When water temperature and pressure reach their critical points (T_c = 374^{o}C, P_c = 22.1MPa), a new state can be found — the supercritical state (Guo *et al*., 2010). Physicochemical characteristics such as ion product, density, dielectric constant and viscosity of water, under supercritical conditions, are totally different from either extreme state, i.e. the gas phase or the liquid phase (Guo *et al*., 2010).

The dielectric constant of water controls the solvent behavior and the ionic dissociation of salts. Accurate experimental data for the dielectric constant over large regions of temperature and pressure has been reported (Weingartner and Franck, 2005). The dielectric constant of water decreases with increasing temperature and increases with increasing density. The high value of the dielectric constant (approximately 80) occurs only in a small region at low temperatures. In a large supercritical region at high densities, the dielectric constant ranges from 10 to 25. These

values are similar to those of dipolar liquids and are sufficiently high to dissolve and ionize electrolytes, but also enable miscibility with nonpolar solutes. At low densities the dielectric constant decreases rapidly and finally reaches a value of about 6 at the critical point and and thus the ability to dissolve and ionize electrolytes decreases (Weingartner and Franck, 2005). The reason for this decrease is the reduced number of hydrogen bonds (Serani *et al*. 2010). The change in dielectric constant can lead to a change in the dissolving capacity of water. As the dielectric constant of supercritical water roughly corresponds to that of common organic compounds, it has good solubility for nonpolar organic compounds (Guo *et al*. 2010). On the contrary, dissolving capacity for highly polar inorganic compounds drops dramatically, which causes separation of dissolved organic compounds out of water (Guo *et al*., 2010).

SCW possesses gas-like viscosity and liquid-like density properties; it has better mass transfer and salvation abilities (Guo *et al*., 2010). The viscosities of gases and liquids differ by about two orders of magnitude under normal conditions. When the density is between 0.6 and 0.9 gcm^{-3}, the viscosity depends only weakly on temperature and density. In this range, the viscosity amounts only to about one tenth of its value under normal conditions (Weingartner and Franck, 2005). This high fluidity is attractive in chemical processes because mass transfer and diffusion-controlled chemical reactions are largely enhanced. With increasing temperature and pressure, the density of water decreases. At the critical point, the density of the liquid and gas phases are equal. Therefore, above the critical point, the density of SCW can be changed continuously by varying pressure and temperature (Serani *et al*. 2010).

Another key property of hot compressed water is the ion dissociation constant (K_w). The ion product is related to both temperature and density, but density has a greater impact. Below the critical point, the higher the density, the higher is the ion product (Weingartner and Franck, 2005). Thermodynamic calculations show that the ion product increases from 10^{-14} for liquid water ($T = 25^oC$, p = 0.1MPa) to around 10^{-11} at near critical conditions ($T = 320^oC$, p = 25MPa); then a decrease is observed as soon as the critical point is crossed ($Kw = 10^{-20.9}$ at $T = 420^oC$, p = 25MPa) (Serani *et al*. 2010). The increasing temperatures result in SCW with high ion concentrations, namely $[H^+]$ and $[OH^-]$. Thus SCW can act like an acid or base catalyst in the reactions. Many organic chemicals that cannot react in water without the presence of strong acid or base catalyst may readily react under the hydrothermal condition of SCW. Lignocellulosic

materials, which are non-polar, become easily hydrolyzed in supercritical water (Basu, 2009).

2.5Reaction Chemistry

The overall chemical reaction for biomass gasification to hydrogen in SCW is endothermic (Guo *et al*., 2007):

$$CH_xO_y + (2 - y)\, H_2O \rightarrow CO_2 + (2 - y + x/2)\, H_2 \quad (2.12)$$

There are three major competing intermediate reactions during the gasification of biomass in SCW (Guo *et al*., 2007):

Steam reforming:

$$CH_xO_y + (1 - y)\, H_2O \rightarrow CO + (1 - y + x/2)\, H_2 \quad (2.13)$$

Water-gas shift:

$$CO + H_2O \rightarrow CO_2 + H_2 \quad (2.14)$$

Methanation:

$$CO + 3H_2 \rightarrow CH_4 + H_2O \quad (2.15)$$

As our desired product for SCWG is H_2, the water-gas shift reaction should be dominant and methanation should be restrained. A high reaction temperature can provide this effect.

SCWG is a process associated with hydrolysis and pyrolysis reactions. Water takes part in the reaction, not only as a reactant but also as a catalyst in the SCWG reaction process (Guo et al., 2010).

2.5.1 Water as a participant in reaction

Under high temperature conditions, the structure of water changes while leads to a reduction in both intramolecular and intermolecular hydrogen bonding. This makes it possible for water to provide hydrogen. In order to prove that high temperature water has the potential to provide hydrogen, research was conducted in 1994 using D_2O as a reaction medium in the hydrothermal

reaction of hydrocarbons, and it was found that hydrogen–deuterium exchange existed in the process and a portion of the deuterium atoms entered into the product (Kuhlmann *et al*. 1994). Research carried out in 2003 used D_2O for the SCWG of some organic compounds using RuO_2 catalyst. The results showed that the methane and hydrogen in gas produced were CD_4 and D_2, which indicated that all the hydrogen in gas product was from D_2O (Park *et al*., 2003).

Water can also produce H_2 through the water-gas shift reaction:

$$CO + H_2O \rightarrow CO_2 + H_2 \tag{2.14}$$

This reaction is weakly exothermic (H = -41 kJ/mol) and thermodynamically limited at the operational temperatures of the process, but allows a significant CO abatement and further hydrogen formation (Corbo *et al.* 2009). Lee *et al*. studied SCWG of glucose without a catalyst (480–750^{o}C, 28 MPa, 10–50s). They observed that CO yield was high in the early stage but when the temperature was over 650^{o}C, because of the beginning of the water-gas shift reaction, CO concentration decreases and H_2 production was enhanced (Lee *et al*. 2002).

2.5.2. Water as a catalyst

Water molecules also participate in SCW reactions as a catalyst. Under SCW conditions, H^+ and OH^- exist in high concentration, which creates conditions favorable to acid–base catalytic reactions.

Acid-catalyzed reaction of organic compounds is available in pure subcritical and supercritical water without any catalyst (Guo *et al*., 2010). Research reported that dehydration of cyclohexene occurs at subcritical conditions without addition of catalyst. With this result, the researchers supposed that the reaction was catalyzed by H_3O^+ generated from water at high temperature. This hypothesis is inconsistent with research which reveals the reaction of tert-butyl alcohol could occur at 250^{o}C in water without addition of any catalyst (Guo *et al*., 2010). Temperature has a great influence on the ionization of water (Serani *et al*., 2010). Water can be an effective acid catalyst at subcritical condition. In addition, Ikushima *et al*. (2000) reported that SCW itself successfully functions as an acid catalyst in accelerating pinacol and Beckmann rearrangements.

Many chemical reactions take place in SCW, while under normal conditions; these reactions

are only possible with the addition of base catalyzed materials. To confirm base catalytic effect of supercritical water, Ikushima *et al*. (2000) conducted an investigation on benzaldehyde disproportionation without catalyst. OH^- ion was required to form the product alcohol in any reaction mechanisms, the participation of the OH^- ion in the disproportionation using SCW was clearly demonstrated (Ikushima *et al.*, 2000). Ethanol and formic acid can be produced from Cannizzaro-type reactions of formaldehyde in subcritical water without catalyst, which is well-known to occur in the presence of a large amount of base catalyst under ambient conditions (Guo *et al*., 2010).

2.6 Effect of parameters

2.6.1 Temperature

Reaction temperature has a significant effect on SCWG especially in the absence of catalyst (Guo *et al*., 2007). A Lee *et al*. (2002) study on SCWG of glucose showed that hydrogen and carbon dioxide yield increased with temperature. The yield of carbon monoxide increased with temperature, but after reaching a maximum level, it dropped rapidly.

In another study, a large effect of temperature on gasification was observed at 25 MPa (Hao *et al*., 2003). With a 30% increase in reaction temperature (500 to 650^oC), the carbon efficiency (CE) and the gasification efficiency (GE) increased by 167% and 300%, respectively, while hydrogen production increased by 46% but CO yield was reduced by 74%.

2.6.2 Water to biomass ratio

Results on gasification of glucose by Matsumura *et al*. (2005) showed that the yields of H_2, CH_4 and CO_2 decreased when the glucose concentration in the feedstock increased, but the yield of CO increased.

Experiments with real biomass carried out in SCW (Vogel and Waldner, 2006, Lu *et al*., 2006 and Guo *et al*., 2007) also showed that at high feed concentrations, both gasification efficiency (GE) and carbon conversion efficiency (CE) were lower. The yields of H_2, CH_4 and CO_2 decreased with increasing biomass concentration, while the yield of CO increased.

2.6.3 Residence time

The reactor residence time is defined as the reactor volume divided by the volumetric flow rate of water at the reactor temperature and pressure. It has an important effect at the beginning, but after reaching a "certain time" it does not change much. This time depends on many factors.

For a batch reactor, residence time is the duration of time that reactants stay inside the reactor. In SCWG of glucose at 374^{o}C, Williams and Onwudili (2005) found that the gasification efficiency increased slightly and reached 90% after 120 min. In experiments with rice husk at 650^{o}C and 30MPa, Basu *et al*., (2009), showed that hydrogen yield increased from 7 to 14mol/kg when residence time increased from 10 to 40 minutes and remained constant up to a residence time of 60 minutes.

2.6.4 Pressure

The effect of pressure on SCWG of biomass is complex. gasification efficiency (GE) and yield of hydrogen and carbon dioxide increased with an increase in pressure at 500^{o}C, while at 650^{o}C the opposite effects were found when glucose was gasified (Hao *et al*., 2003).

Lu *et al*. (2006) found a modest increase in hydrogen yield when the pressure increased from 17 to 30 MPa. Over a wider range of pressures，the GE and carbon efficiency (CE) seemed to be independent of pressure.

2.6.5 Size of biomass particles

In research regarding gasification of rice straw, Lu *et al*. (2006) found that smaller feed particles could improve hydrogen yield, GE and carbon CE during SCWG. As mechanical grinding of biomass to fine particles costs additional energy, an optimal particle size should be found with consideration of economy and feasibility.

2.6.6 Heating rate

Sinag *et al.* (2004) found that a high heating rate generally favors the biomass gasification process in SCW. The results showed that at a higher heating rate, higher yields of hydrogen, methane and carbon dioxide were obtained, but the carbon monoxide yield was low. As the time spent in the subcritical region is short, the formation of coke/char is reduced. Matsumura *et al.*

(2006) noted that tar production decreases with temperature due to the formation of furfural.

2.7 Effect of Catalysts

The use of catalysts has been found to decrease tar and char formation and to increase gas yields. For example, carbon and activated carbon have been used to decrease the formation of residual chars and tars (Matsumura *et al.*1997). Wang and Takarada (2001) studied $Ca(OH)_2$ in coal gasification in SCW and were able to decrease the amount of tar/char, but it has been found that using this type of catalyst can lead to plugging in continuous flow reactors.

To increase the selectivity of hydrogen production, high activation energy is needed for the reaction without catalysts. This leads to high costs of equipment and operation. In recent years, a lot of research has focused on CSCWG with the goal of reducing costs.

2.7.1 Homogenous Catalyst

The main characteristic of alkali metal catalysts in SCWG is to improve the water-gas shift reaction.

Due to the catalytic effect of adding KOH on the water-gas shift reaction, when the content of KOH increased from 0 to 5 wt%, the yield of CO from SCWG of pyrocatechol decreased and the production of H_2 and CO_2 increased (Kruse *et al*., 2000). Formic acid is presumed to be the intermediate product in the reaction process, and the production of H_2 and CO_2 is due to decomposition of formic acid.

$$CO + H_2O \leftrightarrow ``HCOOH'' \leftrightarrow CO_2 + H_2 \qquad (2.16)$$

K_2CO_3 and Trona ($NaHCO_3.Na_2CO_3.2H_2O$) were found to be effective catalysts for the CSCWG of some real compounds such as lignocellulosic materials (Yanik *et al*. 2008). The yield of H_2 increased significantly with these catalysts.

NaOH also has been used as a catalyst in SCWG. In 2003, a research group conducted CSCWG experiments on N-hexadecane and lignin with NaOH at 400 ^{o}C and 30 MPa. With the addition of NaOH, the yield of H_2 was 4 times higher than that without NaOH, while the production of coke was effectively inhibited (Watanabe *et al*., 2003). Kruse *et al.* (2000) investigated SCWG of pyrocatechol with KOH. The smallest yield of CO was obtained and the

H_2 and CO_2 yields increased with an increase in KOH content from 0 to 5 wt%. In 2009, Onwudili and Williams studied SCWG of glucose with NaOH. They found that the hydrogen yield increased dramatically by increasing the sodium hydroxide concentration to 1.67M.

This indicates that alkali catalysts are effective for high hydrogen yield, but they may cause corrosion, plugging or fouling.

2.7.2 Heterogeneous catalysts

2.7.2.1 Transitional metal catalysts

2.7.2.1.1 Ni based catalysts

The cost of nickel catalysts is relatively low, and they have been applied extensively to many petrochemical industries. In recent years, nickel catalysts have been introduced into SCWG system. It was found that Ni can accelerate the conversion of biomass, but both Ni catalyst and its support are unstable. In the meantime, it can cause sintering and deactivation in the reaction process in both batch and continuous-flow experiments. In 2008, research was carried out on the evaluation of catalysts for hydrothermal gasification. The results showed that Ni catalyst was limited by its life performance (<100 h) and both the physical and chemical structure of the catalyst support greatly changed under hydrothermal condition (Elliott *et al*., 2008).

Different supports may have different effects on the activity of Ni catalysts. Furusawa *et al*. employed Ni/MgO as the catalyst for CSCWG of lignin and found that 10 wt% Ni/MgO (873 K) had the best catalytic performance (carbon yield of 30%) (Furusawa *et al*., 2007). The carbon based nickel (Ni/C) catalyst showed high catalytic activity at hydrothermal conditions. In 2008, Elliott *et al*. found that among Cu, Ag, Sn, Ru and some other trace elements as additives, Ru increased the activity of Ni catalyst. Moreover, it had a longer life performance. The gasification of glucose was investigated by Muangrat et al. (2010). It was found that the hydrogen yield was increased by 50% and 100% in the presence of Ni/SiO_2 and Ni/Al_2O_3 catalysts, respectively.

2.7.2.1.2. Ruthenium catalyst.

Ruthenium is a very active catalyst for low temperature catalytic gasification. In CSCWG experiments with glucose, the addition of Ru/Al_2O_3 can improve conversion rate and H_2 yield. Moreover, Ru/Al_2O_3 can inhibit CH_4 production (Byrd *et al*., 2007). Another report also showed

high H_2 selectivity for a Ru catalyst in CSCWG of lignin and glucose at low temperature (400^{o}C). Intermediate compounds such as formaldehyde were decomposed rapidly to CH_4, CO_2 and H_2 with Ru as catalyst. Sato *et al*. (2003) found that in the CSCWG process, the activity order was Ru/γ-Al_2O_3 > Ru/ C > Rh/C > Pt/γ-Al_2O_3, Pd/C and Pd/γ-Al_2O_3.

However, Ru catalyst poisoning is usually caused by a trace amount of S which can exist in biomass in the form of $S^{2-}$and SO_4^{2-} (Osada M *et al*., 2007).

2.7.2.1.3. Other metal catalysts.

Pt-based catalysts have shown high activity and good selectivity for the production of hydrogen in CSCWG of sugars and alcohols at low temperature. The performance of different active metal loadings on SiO_2 followed the order: Pt~Ni > Ru > Rh~Pd > Ir (Davda *et al*., 2003).

2.7.2.2 Activated carbon catalysts

Activated carbon is another catalyst with high catalytic activity for hydrothermal reactions. Furthermore, secondary pollution is not likely to be caused by dissolved metal from the metal catalysts mentioned above.

In the CSCWG process, activated carbon can not only increase carbon gasification efficiency, but also improve the water-gas shift reaction. However, deactivation on carbon gasification occurred after 4 h and the water-gas shift reaction occurred after 2 h (Guo *et al*., 2010). Both AC and Ni/AC were used in a SCWG process for glucose by Lee (2011) at 650^{o}C. The hydrogen yield increased from ~0.3mol/mol of glucose without catalyst to ~ 1mol/mol of glucose with activated carbon as catalyst and to ~4mol/mol of glucose with Ni/AC catalyst.

2.7.2.3 Dolomite and olivine

Dolomite is a carbonate mineral composed of calcium magnesium carbonate $CaMg(CO_3)_2$. Olivine is a mineral with a formula of $(Mg,Fe)_2SiO_4$ (Hu *et al*., 2006, Devi *et al*., 2005). Dolomite and olivine are cheap disposable catalysts and can reduce the tar content of the gas product. However, dolomite is fragile which makes it quite difficult to separate it from the solid products of biomass gasification. It is proven that the catalytic activities of calcined dolomite and calcined olivine are higher than the untreated one for SCWG (Hu *et al*., 2006, Devi *et al*., 2005).

2.7.2.4 Catalysis of reactor wall

One study on the reaction of methanol in SCW in a tubular flow reactor (Inconel 625) was carried out by Boukis *et al*. (2003). The results suggested that the heavy metals of reactor's inner surface had a significant influence on the conversion and the composition of the reaction products (Boukis *et al*., 2003). The inner active surface could accelerate both the water-gas shift reaction and methanol decomposition. Moreover, the catalytic activity would last for more than 1000 h in operation (Boukis *et al*., 2003).

Research carried out by Lee *et al*. (2002) revealed that reactors made of Hastelloy C-276 increased H_2 yield efficiency. Inconel and "new" Hastelloy were both thought to be effective with the water-gas shift reaction, but the "corroded" Hastelloy wall only catalyzed the decomposition of acetic acid.

Yu *et al*. (1993) conducted glucose gasification with both Inconel and Hastelloy reactors. Results indicating that the Hastelloy wall had a better effect in catalyzing the steam reforming reactions than did the Inconel wall. The Inconel reactor seemed to catalyze the water gas shift reaction which in turn produced a gas rich in hydrogen and carbon dioxide, but the gas product of the new Hastelloy reactor was rich in carbon monoxide (Yu *et al*., 1993).

It is proven that carbon buildup on the reactor wall (Hastelloy) during biomass gasification could reduce the catalytic effects of the metallic wall on the gasification chemistry (Antal *et al*., 2000). This means that biomass feedstock can deactivate the reactor wall.

Many researchers studied gasification in batch reactors with catalysts, and Table 2.1 presents a summary of catalysts used in SCWG.

Table 2.1 Summary of catalysts used in biomass gasification in supercritical water (batch reactors)

Reactant	Catalyst	Experimental conditions	Results	Reference
Glucose	Ni/activated charcoal	575-725^{o}C; 28Mpa Conc 0.3-0.9M	Ni/AC showed high hydrogen selectivity and stability	Lee *et al*., 2009
	Ni/CeO2-γAl2O3	400^{o}C; 25.4 Mpa	H_2: 12.7mol/kg biomass	Lu *et al*., 2010
	NaOH	350^{o}C; 21.5Mpa	Hydrogen takes 50% volume of the gas product	Juda A *et al*., 2009
		450^{o}C; 34Mpa	Hydrogen takes 80% volume of the gas product	
Lignin	Ru/TiO2	400^{o}C	Catalyst is poisoned by adding sulfur	Osada M *et al.*, 2007
	Ni/MgO	250-400^{o}C	Gas product increased with increase in nickel loading	Sato T *et al*., 2006
	Cu	600^{o}C	H_2: 2.7mol/kg biomass	Resende and Savage, 2010
	Fe	600^{o}C	H_2: 1.7mol/kg biomass	
	RuO2	400-450^{o}C (2h)	Gasification percent is 7.9%	Zhen F *et al*., 2008
	Ru	400^{o}C (3h)	Gasification percent is 100%	
Cellulose	RuO2	400-450^{o}C (2h)	Gasification percent is 97%	
	Ni	374^{o}C (30min)	Gasification percent is 18%	
	Ni	350^{o}C (30min)	Gasification percent is 84%	

3. Experimental section

3.1 Materials

The glucose and cellulose samples were obtained as dry powders from Sigma-Aldrich (Oakville, ON, Canada) with 95% purity. Sodium hydroxide and potassium hydroxide were also obtained from Sigma-Aldrich and the pellets were crushed into fine particles. The Al_2O_3 and MgO supports were obtained from Alfa Aesar (Ward Hill, MA, USA) and Sigma-Aldrich, respectively. Four kinds of Ni-based catalysts, Ni/Al_2O_3, $Ni/CeO_2/Al_2O_3$, Ni/MgO, and Ni/AC, were used for the supercritical water gasification process. AC is prepared from lignite coal using steam activation at an activation temperature of 707^oC, steam to coal mass ratio of 0.93, and activation time period of 1.1 h (Azargohar and Dalai, 2005). The Ni-based catalysts were prepared by the incipient wetness method (Botchwey 2010). {($Ni(NO_3)_2 \cdot 6H_2O$), ($CeCl_3$)} as the precursor for Ni-based catalyst preparation was obtained from Alfa Aesar with 97% purity. The solvents used in this work were distilled water and HPLC grade acetone purchased from Fisher Scientific (Ottawa, ON, Canada). Pinewood was obtained as shavings from Descharme Lake (In January of 2010), and was crushed into fine particles. Dolomite was obtained as small particles from Green Earth (Saskatoon SK, Canada). Olivine was obtained as small particles from Opta Minerals (Waterdown, ON, Canada).

3.2 Preparation of pinewood

The pinewood shavings were ground to sawdust using a mill grinder. Then the sawdust was sieved to particles 0.12-1mm in diameter. The sieved particles were spread out on a piece of paper and were left for 3 days at ambient conditions to equalize the moisture content. The pinewood particles were stored in an airtight container.

3.3 Preparation of catalyst

Ni-based catalysts were prepared by impregnating support with the aqueous solutions of the catalyst precursor: {($Ni(NO_3)_2 \cdot 6H_2O$), ($CeCl_3$)} using the incipient wetness method to achieve a 10 wt% Ni loading and Ce/Al atomic ratio of 0.035 ($Ni/CeO_2/Al_2O_3$). The amounts of precursors

used were dependent on the compositions of catalysts. A sample of the required amounts of precursors for the catalysts is shown in Appendix A. First, the calculated amount of precursor was dissolved in water to make a solution. Then, a 1-mL syringe was used to impregnate the solution onto the support particles drop by drop. The freshly impregnated catalyst was allowed to equilibrate for 2 h and then dried overnight in an oven at 105^{o}C. The dried catalyst (except Ni/AC) was then calcined in flowing air at 600^{o}C for 4 h to produce stable catalysts. The Ni/AC catalyst was calcined in flowing nitrogen under the same operating conditions. Dolomite and olivine were calcined in flowing nitrogen at 800^{o}C for 1 h to produce stable catalysts.

3.4 Experimental design

The experimental design for glucose, cellulose and pinewood gasification is presented in Table 3.1.

3.4.1 Catalyst control runs

In order to know whether the catalysts were stable and whether the addition of catalyst alone generated gases, control experiments were carried out with only catalyst and water in the reactor.

3.4.2 Gasification of glucose

In the first phase of this work, glucose was gasified at two temperatures (400 and 500^{o}C) and two water to biomass ratios (3:1 and 7:1) without catalyst. Then, four Ni- based catalysts and NaOH were used to study the effect of catalyst on biomass gasification at identical operating conditions with non-catalytic runs.

3.4.3 Gasification of cellulose

Based on the results of the first phase and the effect of operating parameters on H_2 production, the following experimental design was used for cellulose gasification: cellulose was first gasified at three temperatures (400, 470 and 550^{o}C) and two water to biomass ratios (3:1 and 7:1) without catalyst. For catalytic runs, Ni/CeO_2/Al_2O_3, calcined dolomite and KOH were used at identical operating conditions with non-catalytic runs of cellulose.

3.4.4 Gasification of pinewood

Finally, pinewood was gasified at the best operating conditions (temperature: 550^{o}C, water to biomass ratio: 7:1, residence time: 30 min) derived from the cellulose gasification studies with three catalysts: Ni/CeO_2/Al_2O_3, calcined dolomite and KOH.

3.4.5 Other gasification runs

There were some other experiments for glucose and cellulose gasification.

In order to know the net effect of Ni, both Ni/AC and AC were studied at the same operating conditions for glucose gasification.

In order to study the effect of different alkali precursors, NaOH and KOH were studied at the same operating conditions for glucose gasification.

Calcined dolomite and calcined olivine were both used for cellulose gasification at the same operating conditions to compare the effect on H_2 production.

3.5 Experimental Methods

The schematic of the reaction set-up is shown in Figure 3.1. The gasification experiments were carried out in a 6-mL 316 stainless steel batch reactor with an O.D of 0.95 cm (3/8 inch) and a wall thickness of 0.17 cm (0.065 inch) obtained from Swagelok (Saskatoon, SK, Canada).

For the set of non-catalytic runs, 0.65 g of biomass was loaded into the batch reactor, followed by adding 1.95 g or 4.55 g of distilled water, corresponding to two water-to-biomass ratios of 3 and 7, respectively. For catalytic runs, the experiments were carried out for catalytic gasification at identical operation conditions using 0.65 g of Ni based catalysts/dolomite and 1.67M NaOH/KOH.

Before each run, the reactor was first evacuated with a vacuum pump (50 mmHg) for 5 min and then was purged with N_2. This step was repeated for three times to remove air. And finally the reactor was pressurized with N_2 to 10-16.5 Mpa in order to reach 23-25 Mpa at the final operating temperatures.

The reactor was then heated by a furnace with a heating rate of 30^{o}C/min up to the gasification temperatures. After reaching the desired temperature, the reactor was maintained at

Table 3.1: Experimental design for glucose, cellulose and pinewood gasification.

Material	Temperature (^{o}C)	Water to biomass ratio	Catalysts	Total runs
Glucose	400	3:1	Ni/Al_2O_3	2*2*6=24runs
	500	7:1	$Ni/CeO_2/Al_2O_3$	
			Ni/MgO	
			Ni/AC	
			NaOH	
Cellulose	400	3:1	$Ni/CeO_2/Al_2O_3$	3*2*4=24runs
	470	7:1	Dolomite	
	550		KOH	
Pinewood	550	7:1	$Ni/CeO_2/Al_2O_3$	4runs
			Dolomite	
			KOH	

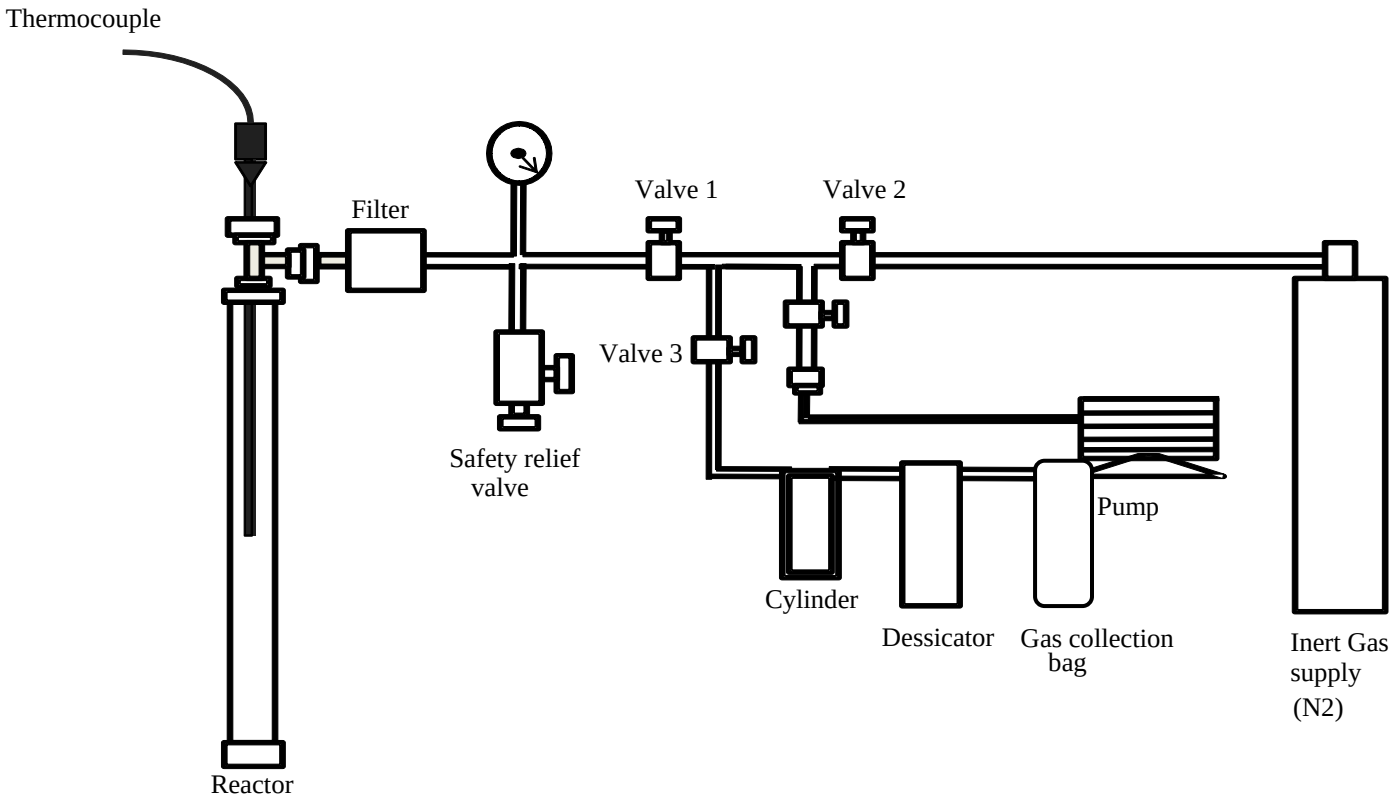

Figure 3.1: Experimental set-up for supercritical water gasification

the operating temperature for 30 min before being cooled rapidly to room temperature by cold water spraying.

3.6 Separation of Reaction Products

After the reactor reached room temperature, the gas product inside the reactor was released into a gas bag through a cylinder to reduce the pressure and a desiccator to capture the moisture. The gas was analyzed with a gas chromatograph (GC).

As shown in Figure 3.2, the liquid and solid products were removed completely from the reactor by rinsing first with distilled water and then with HPLC grade acetone into two clean beakers (liquid phase 1 and liquid phase 2, respectively). Liquid phase 1 was filtered through Whatman No. 2 filter paper to separate the solid phase from the water solution. A rotary evaporator was used for water removal from liquid phase 1 and the resulting product, denoted as "water phase product" was quantified by weighing. It should be noted that, some products of low boiling point may have evaporated during the evaporation process, and this would cause some error in quantifying the water phase yield. Due to water's relatively high boiling point, it is very challenging to quantify the water phase yield accurately. The most widely used method so far is evaporating water under reduced pressure (Xu and Donald, 2008; Xu and Lad, 2008; Qu *et al*., 2003). Liquid phase 2 also was filtered through the same filter paper to separate the solid phase from the acetone solution. The acetone soluble product was recovered by removing acetone under flowing N_2 gas and the resulting product, denoted as "acetone phase product" was quantified by weighing.

The solid residue together with the filter paper was dried overnight in an oven at 105^{o}C before weighing. When the feedstock was pure glucose or pure cellulose, the products were dry and ash free. For catalytic runs, some necessary approximations were made depending on the solubility of the catalysts. For experimental runs with NaOH/KOH (soluble in water), it was assumed that the catalyst essentially remained in the water phase product. So, after quantifying the yield of water phase products, the yield was corrected by excluding the amount of NaOH/KOH added to the reactor. For the experimental runs with Ni-based catalysts/dolomite, due to low solubility in water, the catalysts were assumed to remain in the solid phase. Thus, the yields of solid phase for Ni-based catalysts/dolomite were corrected by excluding the catalyst

amount from the weight of the solid residue. In addition, there is a possibility that the chemical structure of catalysts changed during treatment in supercritical water. For example, in the presence of NaOH/KOH, the CO_2 produced may react with NaOH/KOH and form $NaHCO_3$/$KHCO_3$ (Onwudili and Williams, 2009).

3.7 Characterization Methods

The gas products were collected by a gas bag and were injected into the gas chromatograph (Agilent 7890A) equipped with two TCDs (Thermal conductivity detector), one FID (Flame ionization detector), five packed columns, and one capillary column.

The porous characteristics of all catalysts were measured using nitrogen adsorption technique by an automated gas adsorption analyzer, ASAP 2020 (Micromeritics, Instruments Inc., GA USA). After degassing of samples at 200^{o}C to a vacuum of 550 μm Hg, nitrogen adsorption-desorption isotherms at -196^{o}C were measured by this equipment. The BET surface area was calculated by using the BET equation [18]. For each analysis, ~ 0.2 g of sample was used. The accuracy of measurements performed by this equipment was ± 5 %. The BET surface area of four kinds of catalysts is listed in Table 4.4.

The metal dispersion of catalysts was measured by temperature-programmed CO-chemisorption for fresh calcined catalysts using Micromeritics Pulse Chemisorption Chemisorb 2720. Typically, about 0.2g of catalyst was used in each measurement. In addition, the used catalysts were subjected to temperature programmed evaluation viz. TPO-TPR schemes. Each catalyst was subjected to evacuation with a ramp rate of 10^{o}C/min for 30 min, followed by helium flow through a "U" tube used for analysis. After complete evacuation of the sample, the temperature was increased up to 450^{o}C with a ramp rate of 5^{o}C/min followed by cooling to reach the room temperature at a ramp rate of 10^{o}C/min down to 35^{o}C. Further CO was passed through the catalyst bed in a selected pressure range of 100-700 mm Hg for adsorption and desorption calculations for CO-chemisorption, active metallic sites, and the metallic surface area available with the fresh catalyst.

All the Ni-based catalysts (10 wt%) were prepared by the incipient wetness method. The actual Ni loading was measured by Geoanalytical Laboratories, SRC (Saskatchewan Research Council) using an Inductively Coupled Plasma Mass (ICP-MS) system which provides high-

precision, in situ trace element analysis. Inductively coupled plasma mass spectrometry (ICP-MS) is a type of mass spectrometry which is capable of detecting metals and several non-metals at concentrations as low as one part in 10^{12} (part per trillion). This is achieved by ionizing the sample with inductively coupled plasma and then using a mass spectrometer to separate and quantify those ions.

The catalyst crystalline structure was analyzed by X-ray diffraction using a Brukcer D8 Advance Series equipment. The sample was finely ground and loaded into the aperture of a silicon sample holder. DIFFRAC plus XRD Commander Software system was used to collect the data and Eva database was used for phase identification.

Carbon, hydrogen, nitrogen and sulphur percentages were measured by Elementar Vario EL III. Through quantitative high temperature decomposition, solid substances are changed into gases through combustion. ~4-6 mg of sample was burned at 1150^{o}C and the released gases were separated into their components.

The acetone phase products were analyzed by GC 7890A gas chromatograph equipped with a flame ionization detector (FID) and a 30 m/ 0.25 mm column coated with 0.25 μm film thickness (DB-1 column). Helium was used as the carrier gas at a flow rate of 1.2 mL/min at a column pressure of 22 KPa. Compounds were separated following a linear temperature program of 50- 280^{o}C (10^{o}C/min) and then at 280^{o}C for 10 min. The total run time was 40.5 minutes. The percentage composition was calculated using the peak normalization method. The GC/MS analysis was carried out on a Varian Saturn 2200 GC/MS fitted with the same column and a temperature program as described earlier. MS parameters were set as follows: ionization voltage (EI) 70 eV, peak width 2 s, mass range 40-500 amu, and detector voltage 1.5 V.

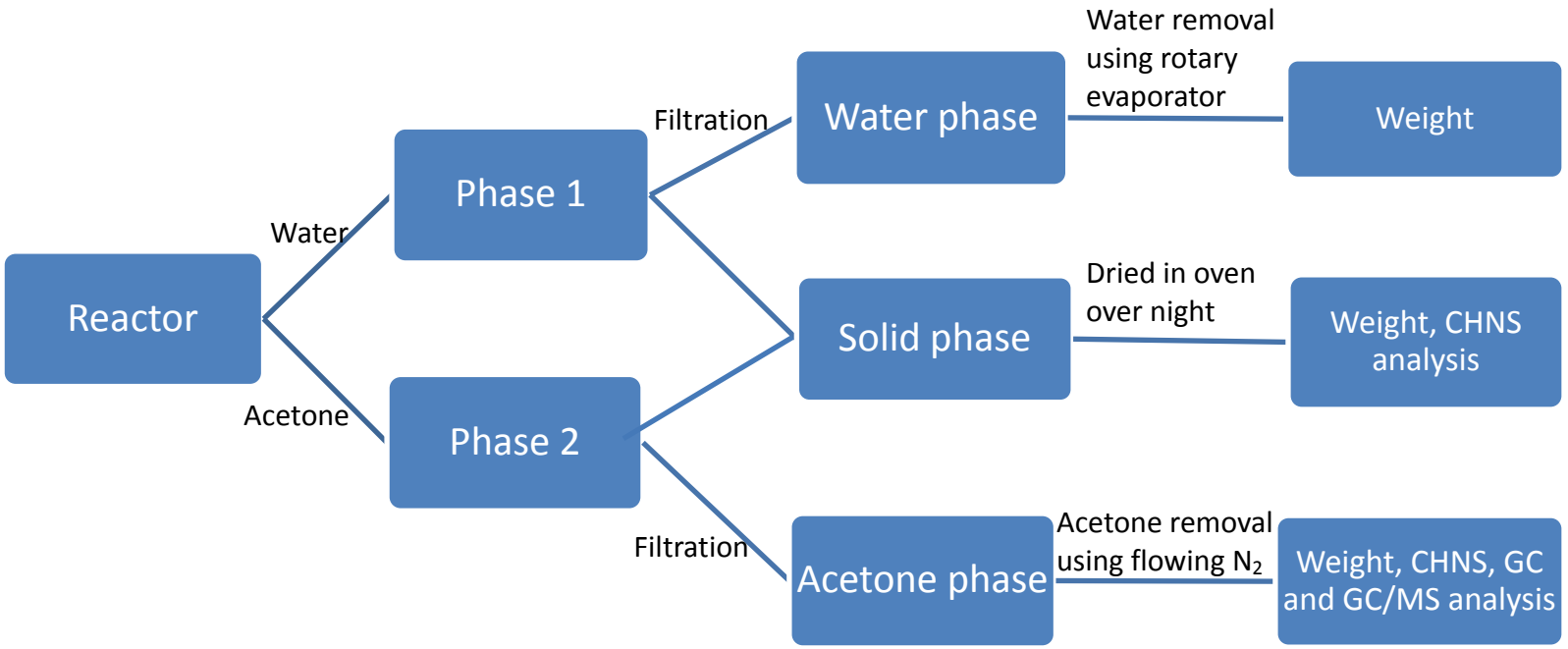

Figure 3.2: Procedures for product collection

4. Results and discussion

4.1 Biomass characterization

Table 4.1 shows the elemental analysis of glucose, cellulose and pinewood. There was no sulfur or nitrogen in glucose and cellulose, and the carbon content was 40 and 42.6wt%, respectively. Pinewood has a higher carbon content at 48.6wt%, with a small amount of nitrogen and sulfur.

Table 4.1 Characterization results of biomass

Material	C	H	N	S	O [a]
Glucose	40.0±0.1	6.9±0.1	0	0	53.1
Cellulose	42.6±0.1	6.6	0	0	50.8
Pinewood	48.1±0.2	6.4±0.1	0.13±0.01	0.2	45.2

[a] *Oxygen (wt%) = 100 wt% – (C + H + N + S) wt%*

In a study by Naik *et al*. (2010), pinewood was subjected to a three-step extraction process: hexane, alcohol and water extraction, separately. The moisture content and ash content of pinewood were also measured. As shown in Table 4.2, pinewood consisted of about 39.0wt% cellulose, 34.0wt% hemicellulose and 12wt% lignin (Naik et al., 2010). As shown in Table 4.3, pinewood contained 5.8wt% moisture and 1.5wt% ash.

4.2 Catalyst characterization

4.2.1Characterization of Ni-based catalysts

Table 4.4 shows the characterization results for Ni-based catalysts. The BET surface area of Ni-based catalysts mainly depends on that of the support. Ni/AC showed the largest surface area of 491m^2/g, while Ni/MgO had the lowest surface area of 5 m^2/g. The loading of Ni caused a slight decrease in surface area of catalyst by blocking some pores. From the ICP results in Table

Table 4.2: Extractives in g from 100g of pinewood (Naik et al., 2010)

Biomass	Hexane extract	EtOH extract	Water extract	Cellulose	Hemicellulose	Lignin
Pinewood	3.6±0.2	6.8±0.3	4.5±0.2	39.0±0.3	34.0±0.3	12.0±0.5

Table 4.3: Proximate analysis of pinewood (Naik et al., 2010)

Biomass	Proximate analysis (wt%)			
Pinewood	Moisture	Ash	Volatile matter	Fixed carbon[a]
	5.8±0.4	1.5±0.2	82.4±0.1	10.3±0.2

[a]% of fixed carbon calculated from difference of moisture, ash and volatile matter content

4.4, the Ni percentage of Ni/MgO was only 1.4%, This was mainly because of the negligible MgO surface area which made the loading of Ni very difficult.

Table 4.4: Characterization results for Ni based catalysts prepared using different supports

Catalysts	BET surface area (m^2/g)	Total pore volume(cc/g)	Ni loading (%)	Ni dispersion (%)
Ni/Al_2O_3	169	0.51	8.2	1.4
$Ni/CeO_2/Al_2O_3$	154	0.44	7.2	1.0
Ni/MgO	5	<0.001	1.4	1.5
Ni/AC	491	0.37	9.9	0.6

4.2.2 Characterization of dolomite

Results from ICP analysis of calcined dolomite, converted to wt% is shown in Table 4.5. After calcination, the predominant components were CaO and MgO. Thus, a 1:1 ratio for both Ca:O and Mg:O was used for calculating of oxygen wt%. There was also some trace amount of other metals detected by ICP, for example, Na, P, Al, Ni, Cu, Zn, Mn *et al*. These compounds may exist as crystalline phases and could promote cracking, polymerization and isomerization reactions (Satterfield, 1991).

X-ray diffraction analysis of the calcined dolomites is shown in Figure 4.1 on the following page. CaO and MgO phases were detected by comparison with a database of standard peaks. Peaks for iron and other trace compounds were not apparent. As discussed before, the ICP result proved the presence of trace amount of iron, alumina and potassium oxide in dolomite. These compounds must have been well dispersed in the sample and therefore beyond the detection limit of the XRD equipment used for this analysis.

Table 4.5: Elemental composition of calcined dolomite

Material	Ca (wt%)	Mg(wt%)	Fe(wt%)	O[a](wt%)	Total[b](wt%)
Dolomite	41.1	19.6	0.57	29.1	90.4

[a] *Theoretical oxygen content calculated from Ca and Mg to represent CaO and MgO species*
[b] *Total wt% accounted for including theoretical oxygen content*

4.3 Study of residence time

Five residence times (10 min 20 min, 30 min, 40 min and 60 min) were used for glucose gasification at 400^{o}C with water to biomass ratio of 3:1. From Figure 4.2, the yield of gas productd increased with an increase in residence time from 10 min to 30 min and then remained steady until 60min. Therefore, a residence time of 30 min was used for this project.

4.4 Non-catalytic gasification of glucose and cellulose

Non-catalytic gasification of glucose was carried out at two temperatures (400 and 500^{o}C) and two water to biomass ratios (3:1 and 7:1) and non-catalytic gasification of cellulose was carried out at three temperatures (400, 470 and 500^{o}C) with the same water to biomass ratios (3:1 and 7:1). The objective of these two sets of experiment was to study the effect of temperature and water to biomass ratio on SCWG of glucose and cellulose.

Table 4.6 shows the yield of glucose gasification products in supercritical water at two temperatures and two water to biomass ratios for non-catalytic processes. As shown in Table 4.6, the products from non-catalyst glucose gasification consisted of ~ 8-17wt% gas, 21-24wt% solid phase, 9-16wt% acetone phase and 8-10wt% water phase. Table 4.7 shows the yield of cellulose gasification products in supercritical water at three temperatures and two water to biomass ratios for non-catalytic processes. As shown in Table 4.7, the products from non-catalyst cellulose gasification consisted of ~ 8-17wt% gas, 17-34wt% solid phase, 8-14wt% acetone phase and 8-12wt% water phase.

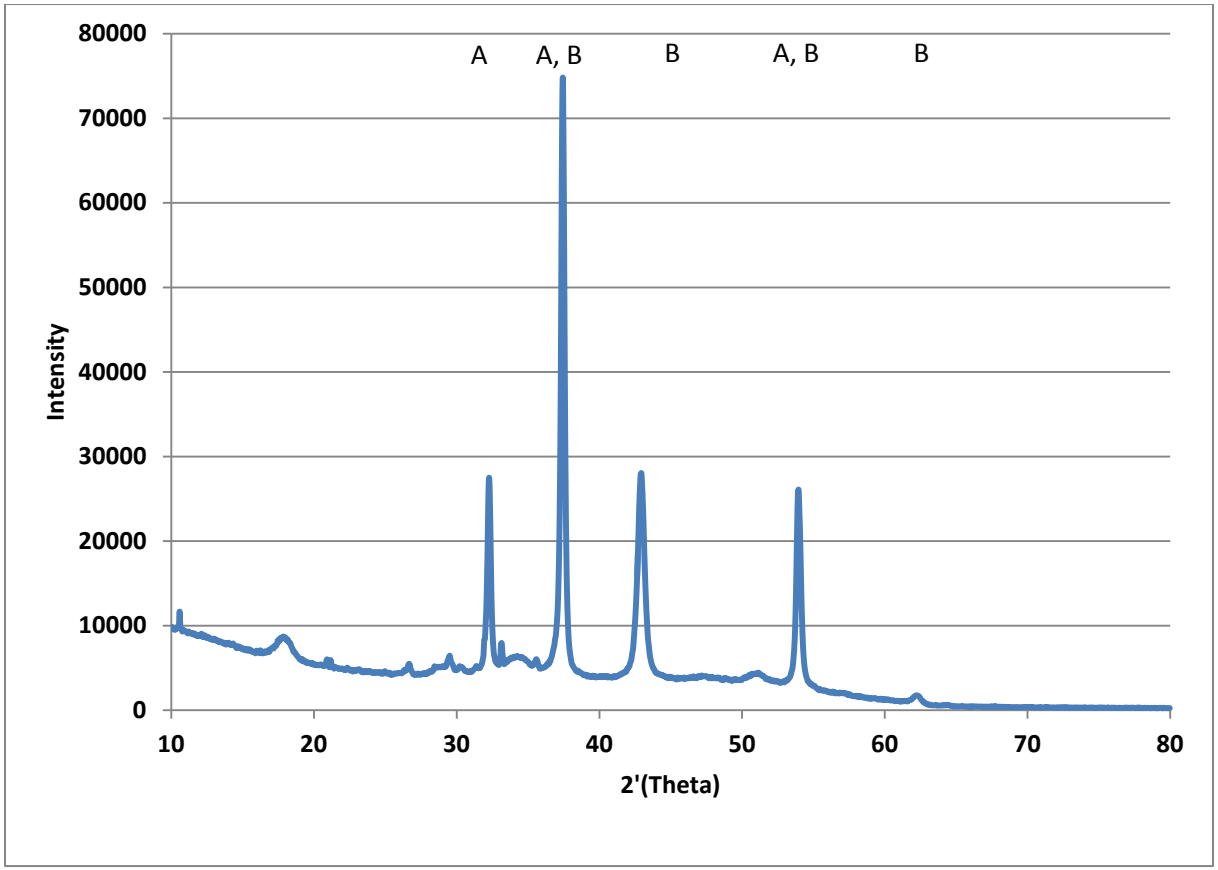

Figure 4.1: X-ray diffraction patterns of calcined dolomite (A-CaO, B-MgO)

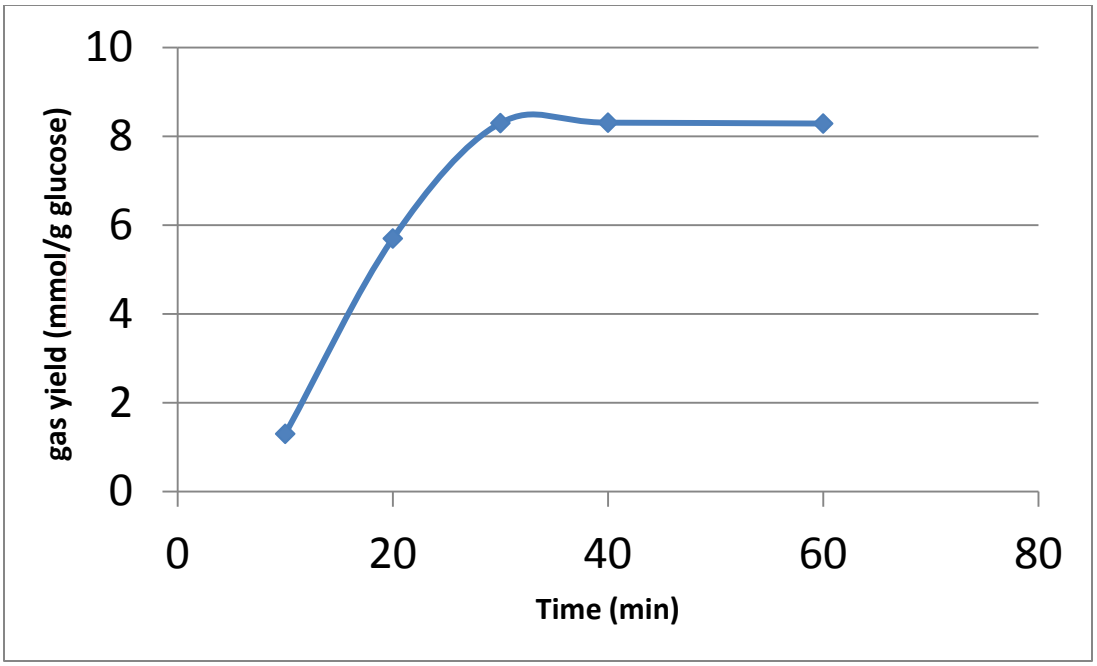

Figure 4.2: Study of residence time for glucose gasification at 400^{o}C with a water to biomass ratio of 3:1

Table 4.8 presents yields of different gas species produced by glucose gasification at two water to biomass ratios and two process temperatures for a residence time of 30min. The yields of H_2, CH_4 and CO_2 increased with an increase in operating temperature. At a water to biomass ratio of 7:1, the yields of H_2, CH_4 and CO_2 higher than those at water to biomass ratio of 3:1. The LHV of gas product and CE (carbon efficiency) are also presented in Table 4.8. The lower heating value (LHV) refers to the amount of heat released by combusting a specified quantity of fuel (initially at 25°C) and returning the temperature of the combustion products to 150°C, which assumes that the latent heat of vaporization of water in the reaction products is not recovered (Sheng and Azevedo, 2005). Table 4.9 shows yields of different gas species produced by cellulose gasification at two water to biomass ratios and three process temperatures for a residence time of 30 min. The yields of H_2, CH_4 and CO_2 were increased with an increase in operating temperature and with an increase in water to biomass ratio.

4.4.1 Effect of temperature

Many researchers have demonstrated that temperature is the most important parameter for a biomass gasification process in supercritical water especially in the absence of catalyst (Guo *et*

al., 2007; Schuster *et al*., 2001; Lee *et al.,* 2002). Generally, the gas product amount increases and the solid yield decreases with an increase in process temperature. During biomass gasification in supercritical water, the gaseous products are mainly produced from steam reforming reactions of liquid and solid products and from decarboxylation and cracking or fragmentation reactions of the liquid products (Antal *et al.,* 2000). In this work, Table 4.6 shows that at a 3:1 water to biomass ratio with an increase in temperature from 400 to 500^{o}C, as expected the gas phase product yield increased from 8.3 to 13.2wt% and the acetone phase product increased from 13.4 to 15.5wt%, while the solid phase and water phase product yields decreased with a temperature increase from 400^{o}C to 500^{o}C. The same trend was found in Table 4.7, which shows the results of cellulose gasification in supercritical water. This indicated that higher temperature can enhance steam reforming, cracking and decarboxylation reactions of liquid and solid products.

Table 4.8 presents yields of different gas species produced with glucose gasification at two water to biomass ratios and two process temperatures for a residence time of 30min. From Table 4.8, all the gas products yields increased by an increase in process temperature and in water to biomass ratio. For both water to biomass ratios, the yield of all gas species in Table 4.8 and Table 4.9 increased with an increase in operating temperature. Similar results have been reported in many other papers studying supercritical water gasification. Hao et al. (2003) showed the significant effects of process temperature for SCWG at 25 MPa; with a 30% increase in reaction temperature (500 to 650^{o}C), the CE increased by 167%, and hydrogen production increased by 46%, but CO yield was reduced by 74%. Carbon efficiency is defined on a dry ash free basis as follows:

CE = carbon in the gas product/carbon in the feedstock*100% (Hao *et al*., 2003).

From Table 4.8, at an operating temperature of 500°C, the yields of H_2 and CO_2 were 0.58 mmol/g and 2.21 mmol/g, respectively, when the water to biomass ratio was 3:1, and the yields of H_2 and CO_2 were 0.77 mmol/g and 2.23 mmol/g when the water to biomass ratio was 7:1. Similar results was presented by Lee *et al*. (2002) for glucose gasification at 480°C, while the H_2 yield was 0.44 mmol/g while the yield of CO_2 was 2.20 mol/g.

The lower heating values (LHV) of gas products were also calculated and presented in Table 4.8 and Table 4.9. Dry product gas lower heating value, LHV (kJ/Nm^3) is calculated using equation (4.1):

$$LHV = (30.3*CO+25.7*H_2+85.4*CH_4+151.3*C_nH_m)*4.2\ (kJ/Nm^3) \quad (4.1)$$

where CO, H_2, etc. are the gas component concentrations in the product gas (Lv *et al*., 2004).

In this work, when the temperature was increased from 400 to 500^{o}C for glucose gasification, the CE increased by 78.9% at a 3:1 water to biomass ratio and 77.4% at a 7:1 water to biomass ratio. For cellulose gasification, the CE increased by 182% at 3:1 water to biomass ratio and 227% at a 7:1 water to biomass ratio when the temperature was increased from 400 to 550^{o}C.

The LHV of the gas product without catalyst was calculated and listed in Table 4.8 and Table 4.9. LHV of the gas product increased with an increase in temperature. LHV of gas product derived from glucose and that from cellulose with catalysts was calculated to be in the range of 60.6-143 kJ/Nm^3 and 74.6-198 kJ/Nm^3, respectively.

4.4.2 Effect of water to biomass ratio

In this study, the water to biomass ratio was varied to investigate the effects of this parameter on product yield for the gasification process. As shown in Table 4.6 and Table 4.7, the runs carried out at 400^{o}C and a water to biomass ratio of 3:1, the yields of solid phase and acetone phase were larger than those at a water to biomass ratio at 7:1, while the yields of the gas and water phase were lower. The same trend can be observed from the other runs carried out at 500^{o}C for glucose gasification and those carried out at 470 and 550^{o}C for cellulose gasification. Similar results were reported by Xu and Donald (2008) which was focused on peat gasification in subcritical and SCW. They observed a larger yield of the acetone phase, but a smaller yield of the water phase and a negligible change in the total gas yield at a lower water to biomass ratio. From the results in Table 4.6, it is likely that with a lower water to biomass ratio, the solvolysis or hydrolysis of glucose might be restricted, which leads to a smaller yield of the water phase and higher yield of solid phase (Xu and Donald, 2008). Furthermore, a higher biomass concentration might promote dehydration reactions of the water phase products and lead to greater yield of the acetone phase (Xu and Donald, 2008).

Water can suppress tar or char formation by solvation and dilution. This is due to the intermediates of biomass gasification, which often have double bonds, dissolved in SCW (Kruse, 2008). The solid product of biomass gasification is mainly from polymerization reactions and is reduced under SCW conditions because of the lower probability to meet. The collision frequency of a single organic molecule with water is much higher than that with a second organic molecule (Kruse, 2008). Meanwhile, the intermediates dissolved in water can react with water or can be catalyzed by OH^- or H_3O^+ ions to split into other compounds, thus improving the degradation of tar components.

However, water can accelerate biomass depolymerization by hydrolysis. The glycosidic bonds of cellulose and hemicellulose are polar and hydrolyzed very rapidly in SCW (Kruse, 2008). In SCW, cellulose and hemicellulose are first split up into sugar units and the entire biomass structure breaks down rapidly. This improves further attack by water molecules which in turn promotes the reaction rate.

The effect of water to biomass ratio on various gas species yields is shown in Table 4.8 and Table 4.9. For glucose and cellulose gasification, water to biomass ratio had a negligible effect on the yield of $C_2+C_3+C_4$, and the yield of CH_4 and CO_2 increased slightly with an increase in water to biomass ratio. When the water to biomass ratio increased from 3:1 to 7:1, the H_2 yield for glucose gasification was increased by 40% and 33% at 400 and 500^{o}C, respectively and the H_2 yield of cellulose gasification was increased by 44%, 11% and 22% at 400, 470 and 550^{o}C, respectively. Similar results were reported by Hao *et al*. (2003) where glucose was used as a model biomass for studying the SCWG, and the results showed that the percentages of hydrogen and carbon dioxide in the total product gas increased with an increase in glucose concentration in the range of 0.1M to 0.9M, while the carbon monoxide and methane fractions were reduced. Furthermore, results for gasification of glucose reported by Matsumura et al. (2005) showed that the yields of H_2, CH_4 and CO_2 decreased at a low water to biomass ratio, while the yield of CO increased. Experiments with real biomass carried out by Guo *et al*. (2007) also showed that the yields of H_2, CH_4 and CO_2 decreased with increasing biomass concentration while the yield of CO increased.

At high temperature, the structure of water is changed; therefore, it is possible for water to provide hydrogen (Guo *et al*., 2010). SCWG research was conducted using D_2O instead of H_2O

as a reaction medium and it was found that hydrogen-deuterium exchange existed in the process and a portion of the deuterium atoms entered the product (Park *et al*., 2003). This demonstrated that water is a source of hydrogen in the SCWG process.

Under supercritical conditions, water acts as an effective medium for the radical reactions which are required for forming gases. At high temperatures, water can also produce H_2 and CO_2 through the water gas shift reaction:

$$CO+H_2O \rightarrow CO_2+H_2 \quad (2.14)$$

This explains the increment of H_2 and CO_2 yields when treating glucose at a higher water to biomass ratio.

Table 4.6: Product yields of glucose gasification (wt%) vs. process temperature and water to biomass ratio for non-catalytic gasification.

Water to biomass ratio	3:1		7:1	
Temperature (^oC)	400	500	400	500
Gas phase yield	8.3±0.2	13.2±0.3	11.2±0.2	16.4±0.3
Solid phase yield	24±0.1	23	22	21±0.1
Acetone phase yield	13.4±0.1	15.6±0.2	9.4	11.5±0.2
Water phase yield	9.2±0.1	8±0.1	9.8±0.1	9.1

Table 4.7: Product yields of cellulose gasification (wt%) vs. process temperature and water to biomass ratio for non-catalytic gasification.

Water to biomass ratio	3:1			7:1		
Temperature(^{o}C)	400	470	550	400	470	550
Gas phase yield	8.9±0.2	9.3±0.1	12±0.1	10.8±0.1	15.2±0.2	16.4±0.1
Solid phase yield	33.8±0.2	30.8±0.1	21.5±0.2	27.7±0.3	24.6±0.2	16.9±0.2
Acetone phase yield	13±0.1	13.5±0.2	14.2±0.2	8.2±0.1	9.3±0.2	10.7±0.2
Water phase yield	9.9±0.2	9.3	8.2±0.1	11.8±0.2	10.6±0.2	10±0.1

Table 4.8: Effects of process temperature on gas component yields (mmol/g of biomass), lower heating value (LHV) (kJ/Nm^3) and carbon efficiency (CE) (%) for non-catalyst runs of glucose.

Water to biomass ratio	3:1		7:1	
Temperature (^oC)	400	500	400	500
H2	0.52±0.02	0.58±0.02	0.73±0.01	0.77±0.02
CH4	0.04	0.52±0.01	0.07	0.57±0.02
CO2	1.84±0.06	2.21±0.11	1.87±0.08	2.23±0.10
CO	0	0.47±0.01	0	0.52±0.01
C2+C3+C4	0.09	0.11	0.10	0.12
LHV (kJ/Nm^3)	34.6	97.3	58.3	97.6
CE (%)	9.0	16.1	11.4	16.5

Table 4.9: Effects of process temperature on gas components yield (mmol/g of biomass), lower heating value (LHV) (kJ/Nm^3) and carbon efficiency (CE) (%) for non-catalyst runs of cellulose.

Water to biomass ratio	3:1			7:1		
Temperature (^oC)	400	470	550	400	470	550
H_2	0.50	0.72±0.01	0.95±0.02	0.72±0.02	0.80±0.02	1.16±0.03
CH_4	0.04	0.09	0.78±0.02	0.06	0.33	0.82±0.01
CO_2	1.52±0.05	1.83±0.04	2.26±0.09	2.19±0.10	2.53±0.07	2.88±0.11
CO	0	0	0	0	0	0
$C_2+C_3+C_4$	0.04	0.13	0.20	0.03	0.04	0.19
LHV (kJ/Nm^3)	36.6	76.6	121	47.7	51.0	107
CE (%)	7.2	10.2	20.3	7.5	15.1	24.5

4.5 Catalytic gasification of biomass

4.5.1 Control experiments

Control experiments were carried out with just the catalyst and water in the reactor. For each control run, 0.65 g of Ni-based catalyst/dolomite was used and the concentration of NaOH/KOH was fixed at 1.67M at 500^{o}C with a water to biomass ration of 7:1 for 30 min. Table 4.10 shows that a small amount of H_2 was formed with only Ni-based catalyst/dolomite and water. This was caused by oxidization of the Ni in supercritical water. Also, there was some CO_2 formed with Ni/AC and water, this was because the reaction between C and water.

Table 4.10: Control experiments with catalysts and water at 500^{o}C and a water to biomass ratio of 7:1 for 30min.

Catalysts	Ni/Al_2O_3	$Ni/CeO_2/Al_2O_3$	Ni/MgO	Ni/AC	NaOH	Dolomite	KOH
H_2 (mmol)	0.008	0.008	0.007	0.012	0	0.009	0
CO_2 (mmol)	0	0	0	0.056	0	0.035	0

4.5.2 Catalytic gasification of glucose

Catalytic gasification of glucose was carried out at the identical operating conditions used for the non-catalytic gasification runs. Four kinds of Ni-based catalysts (Ni/Al_2O_3, $Ni/CeO_2/Al_2O_3$, Ni/MgO and Ni/AC) and one alkali catalyst (NaOH) were studied during this phase of experiments.

For each run, 0.65 g of Ni-based catalyst was used with the same weight of biomass. Due to previous studies showing that the hydrogen concentration significantly increased with increasing NaOH concentration up to 1.67M (Onwudili and Williams, 2009), the concentration of NaOH was fixed at 1.67M in this study.

The mass balance obtained for this set of experiments with catalyst was in the range of 60-76% (Figure 4.3). The unaccounted portion of the original material may largely be due to water loss and evaporation of products during the water removal process when the water phase product was

recovered. In theory, total carbonization of glucose would lead to a 60% weight loss of glucose as shown by: $C_6H_{12}O_6 \rightarrow 6C + 6H_2O$ (Onwudili and Williams, 2009). As mentioned earlier, due to water's relatively high boiling point, it is challenging to quantify the yield of the water phase. Xu and Donald (2008) obtained a mass balance of 67-82wt% in terms of total yield of organics during treatment of peat in supercritical water at 410^{o}C (Xu and Donald, 2008). In the meantime, the small amount of glucose involved in each run made the product collection and recovery quite difficult; this also influenced the mass balance.

4.5.2.1 Effect of NaOH

From Figure 4.3, the results for the non-catalytic process showed that at 500^{o}C, about 15.6% w/w of glucose was extracted into acetone, while 8% w/w of water soluble product was recovered from the liquid product. 13.2% w/w gas was formed, while about 23% w/w of products was converted into char. As shown in Figure 4.4, among all the catalysts, NaOH had the best activity for improving H_2 formation, i.e. the H_2 yield increased by 135% using NaOH as catalyst. Alkali catalysts are easily miscible with water and are very effective for biomass gasification in supercritical water. Alkali compounds such as NaOH, KOH, K_2CO_3, Na_2CO_3 and CsOH have been used as catalysts in biomass gasification process to suppress the formation of char and to enhance the yield of gas and liquid phase products (Guo *et al*., 2010). SCWG of pyrocatechol with KOH was studied by Kruse *et al*. (2000). It was found that the H_2 and CO_2 yields increased with an increase in KOH content from 0 to 5%. Onwudili and Williams (2009) reported the results of SCWG of glucose with NaOH; the hydrogen yield increased dramatically with increasing sodium hydroxide concentration up to 1.67M (Onwudili and Williams, 2009). K_2CO_3 and Trona ($NaHCO_3 \cdot Na_2CO_3 \cdot 2H_2O$) were used for SCWG research as some real biomass materials such as lignocellulosic materials (Yanik *et al*., 2008). It was found that the yield of H_2 increased significantly with the use of catalysts. In this work, as expected, the presence of 1.67M NaOH dramatically improved organic conversion, as the char yield was reduced from 23wt% without catalyst to about 14wt% with NaOH. The use of NaOH increased the yield of gas and had a negligible effect on the acetone phase, and NaOH produced the highest water phase yield at about 26wt% among all five catalysts. NaOH can scour the reactor surface and act as a surfactant and, thus prevent the adherence of particles to the walls of the reactor (Onwudili and Williams, 2009). This is demonstrated in Figure 4.3, where NaOH effectively eliminated the

formation of the solid phase. It is proven that during glucose gasification with NaOH, [$C_6H_6O_6{\cdot}Na_6{\cdot}9H_2O$] was formed at 200 to 300^oC, which can be decomposed to NaCOOH and hydrogen at 350^oC (Onwudili and Williams, 2009). Sinag *et al*. (2004) proposed the reaction between NaCOOH and water to form hydrogen and sodium bicarbonate, while Yu and Savage (1998) proposed that NaCOOH could be decomposed through dehydration or decarboxylation.

The overall equation suggested for SCWG using NaOH is as follows (Onwudili and Williams, 2009):

$$C_6H_{12}O_6 + 6NaOH + 6H_2O \rightarrow 6NaHCO_3 + 12H_2 \quad (4.2)$$

The overall equation shows the possibility that the hydrogen was produced not only from hydrogen atoms in glucose but also from water (Onwudili and Williams, 2009). The high yield of the water phase may be due to the formation of $NaHCO_3$. As mentioned in the products separation part (section 3.6), the weight of the water phase was corrected by excluding the weight of NaOH.

4.5.2.2 Effect of Ni-based catalysts

As shown in Figure 4.4, in the presence of Ni/Al_2O_3, the char formation was reduced to about 14 wt% and the yields of the water phase and the gas phase increased, while the acetone phase yield decreased slightly compared with the non-catalyst run. The run with $Ni/CeO_2/Al_2O_3$ showed similar results as Ni/Al_2O_3, but with slightly larger yields of gas and char. In addition, the yield of the acetone phase was slightly suppressed. The surface acidity of Al_2O_3 was decreased by adding Ce and this modification suppressed the formation of carbon filaments on nickel surfaces significantly and thus maintained the product selectivity of Ni/Al_2O_3 (Sánchez-Sánchez *et al*., 2007). In the presence of Ni/MgO, the water phase and solid phase yields decreased while the yields of other two phase increased. Except for Ni/AC, which made some contribution to solid phase formation, the run with Ni/MgO had the highest solid phase yield of the catalysts, and it was the only catalyst that suppressed the water phase yield. As shown in Figure 4.4, the yield of H_2 was dramatically increased with Ni-based catalysts, and the presence of Ni/AC contributed to an 81% increase in H_2 yield, followed by 62% with Ni/MgO, 60% with $Ni/CeO_2/Al_2O_3$ and 52% with Ni/Al_2O_3. The results indicate that the presence of Ce improved the activity of Ni/Al_2O_3.

As reported by Sato *et al*. (2006), in the presence of MgO only, the total gas yield was below 5 %, while the solid products were formed in 99% yield which was significantly larger than those obtained without catalyst. MgO catalyzed reactions led to the formation of solid products (char or tar). It is proven that the yield of gases increased with an increase in the amount of metal supported on the catalyst; the total gas yields were 21.7, 25.1, and 35.5% with 10, 15, and 20 wt% of Ni/MgO catalyst, respectively (Sato *et al*., 2006). The MgO catalyzed reactions led to unstable lignin fragments which could condense to solid products regardless of the existence of water. In other words, MgO did not promote the formation of lower molecular weight components such as gases. The total gas yield was found to be increased with an increase in nickel loading on the support in the presence of water (Sato *et al*., 2006). Considering the role of the Ni/MgO catalyst, the MgO part effectively promoted the decomposition of lignin to high molecular weight fragments at temperatures of 250 to 350^{o}C (Sato *et al*., 2006). With increasing temperature, the yield of char or tar decreased with an increase in the yield of gases. Thus, the high-temperature region was preferred for reaction between species derived from lignin and water to form gases in the presence of nickel (Sato *et al*., 2006).

4.5.3 Catalytic gasification of glucose with activated carbon and KOH

Activated carbon can act as a catalyst during the SCWG process. As reported by Lee *et al*. (2011) for glucose gasification at 650^{o}C, H_2 yield increased from ~0.3mol/mol of glucose without catalyst to ~ 1mol/mol of glucose with AC. In this work, to study the net effect of Ni, AC and Ni/AC were used at 500^{o}C with a water to biomass ratio of 7:1 for 30 min, the results showed that hydrogen production increased by 6.9% with activated carbon and 36.9% with Ni/AC, while the carbon dioxide yield increased by 94.2% with activated carbon and 124.2% with Ni/AC. The run with activated carbon produced a higher yield of the solid phase at 25.4 wt% compared with 20 wt% with Ni/AC.

To study the effect of different alkali precursors, KOH and NaOH were used at the same operating conditions. The hydrogen yield increased by 312% with KOH and 180% with NaOH. The run with KOH had a 5.4wt% larger yield of char and a 4.6wt% smaller yield of the acetone phase compared to those with NaOH.

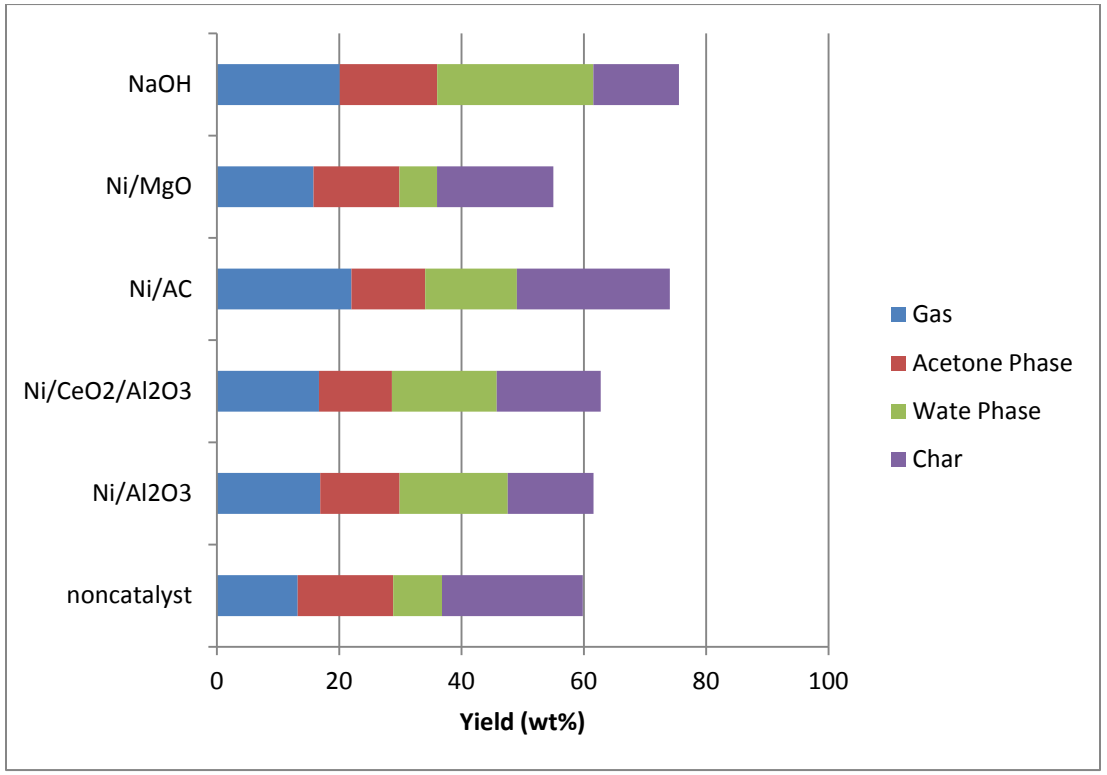

Figure 4.3: Effects of catalysts on product yields (wt%) for 0.65 g glucose gasification carried out with 1.95 g H_2O and 0.65 g Ni-based catalyst or 0.13 g NaOH at 500^oC

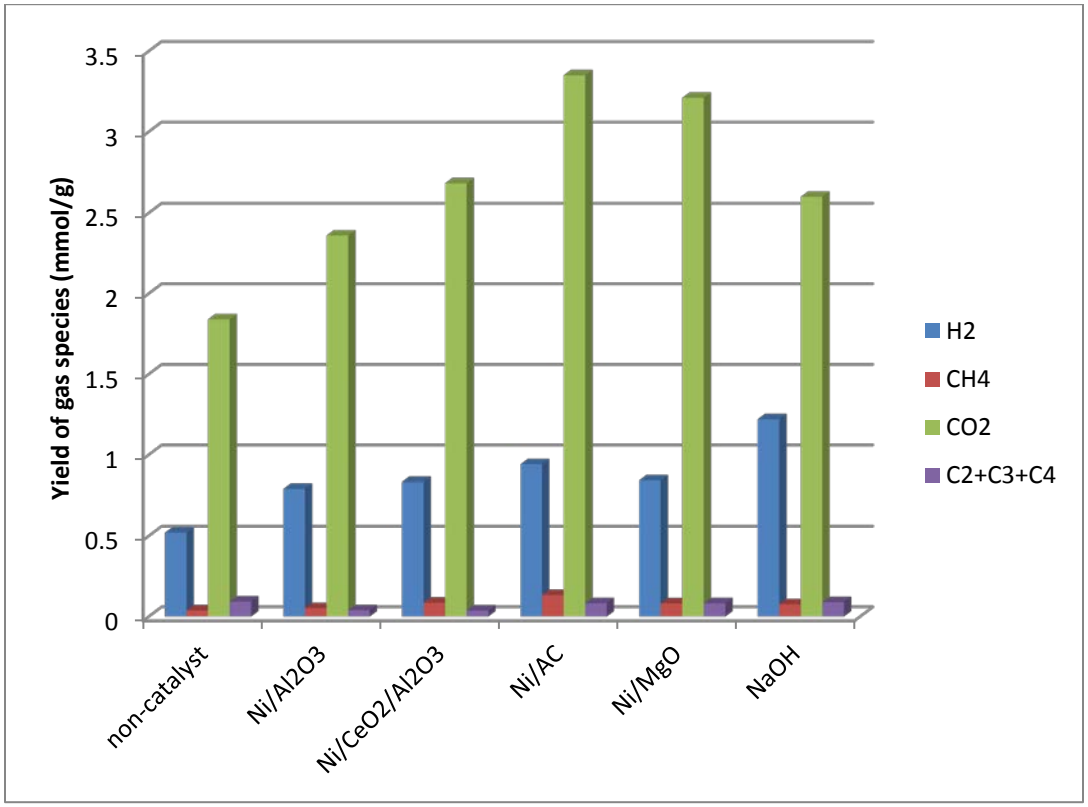

Figure 4.4 Yields of gas species (mmol/g glucose) for SCW treatment of glucose (water to biomass ratio of 3:1) for 30 min at 400^{o}C with various catalysts.

4.5.4 Catalytic gasification of cellulose with calcined dolomite and calcined olivine

Both calcined olivine and calcined dolomite were used as additives in biomass gasification in a fluidized bed. Dolomite was more active for in-bed tar elimination than was raw olivine (Corella *et al*., 2004). The better performance of dolomite was proven in this work. Calcined dolomite and calcined olivine were used as catalysts for cellulose gasification at 400^{o}C with a water to biomass ratio at 3:1. The H_2 yields were 0.916 and 0.824 mmol/g of cellulose in the presence of dolomite and olivine, respectively. Thus, dolomite was studied at various operating conditions for cellulose and pinewood gasification, and its performance was compared with that for other catalysts.

4.5.5 Catalytic gasification of cellulose

Catalytic gasification of cellulose was carried out at the identical operating conditions used for the non-catalytic gasification runs (section 4.4). Three catalysts, Ni/CeO_2/Al_2O_3, calcined dolomite and KOH, were studied during this phase of experiments. For each run, 0.65 g of Ni-based catalyst/dolomite was used with the same weight of biomass, while the concentration of KOH was fixed at 1.67M in this study.

Figure 4.5 shows the effects of catalysts on product yields (wt%) for 0.65g cellulose gasification carried out with 4.55 g H_2O and 0.65 g solid catalyst (Ni/CeO_2/Al_2O_3 or dolomite) or 0.42g KOH at 550^{o}C. Figure 4.6 shows yields of gas species (mmol/g cellulose) for SCW treatment of cellulose (water to biomass ratio of 3:1) for 30 min at a 400^{o}C with various catalysts.

4.5.5.1 Effect of catalysts

As shown in Figure 4.5, the mass balance falls in the range of 60-77wt%. From Figure 4.4, the results for non-catalytic processes showed that at 550^{o}C, about 16% w/w of cellulose was extracted into acetone, while 10% w/w of water soluble product was recovered from the liquid product. 16.4% w/w gas was formed, while about 16.9% w/w of products was converted into char. From Figure 4.6, the non-catalytic run of cellulose has a 0.5 mmol/g H_2 yield and a 1.52 mmol/g CO_2 yield.

As shown in Figure 4.5, in presence of KOH the gas yield was increased from 16.4% w/w without catalyst to 38.4% w/w, and the solid product formation was reduced from 16.9% w/w without catalyst to 1% w/w. The gas yield was increased from 16.4% w/w without catalyst to 24.4% w/w using $Ni/CeO_2/Al_2O_3$, while the yield of solid product was reduced from 16.9% w/w without catalyst to 12.3% w/w using $Ni/CeO_2/Al_2O_3$. As shown in Figure 4.6, among all the catalysts, KOH had the best activity for improving H_2 formation, i.e. the H_2 yield increased by 194% with the use of KOH as catalyst. The presence of $Ni/CeO_2/Al_2O_3$ contributed to an 82.2% increase in H_2 yield.

Calcined dolomite had a quite different effect on cellulose gasification compared with the other two catalysts. As shown in Figure 4.5, the gas yield decreased from 16.4% w/w without catalyst to 9.5% w/w using calcined dolomite, while the yield of solid product increased from 16.9% w/w without catalyst to 31.5% w/w using calcined dolomite. In the meantime, Figure 4.6 shows that the presence of calcined dolomite increased the yield of H_2 from 0.5 mmol/g without catalyst to 0.9 mmol/g.

Calcined dolomite can eliminate unwanted tar and absorb CO_2 during biomass gasification (Corella *et al.*, 2004). This caused the low concentration of CO_2 in the gas product when using calcined dolomite as a catalyst, and caused the high yield of solid product. As mentioned in section 3.6, some necessary approximations were made for catalytic runs depending on the solubility of catalysts. When using calcined dolomite as a catalyst, due to its low solubility in water the catalyst was assumed to remain in the solid phase. Thus, the yield of solid phase was corrected by excluding the catalyst amount from the weight of solid residue. But the calcined dolomite may absorb CO_2 during the gasification process and form carbonate which would contribute to a weight increase in the solid phase product.

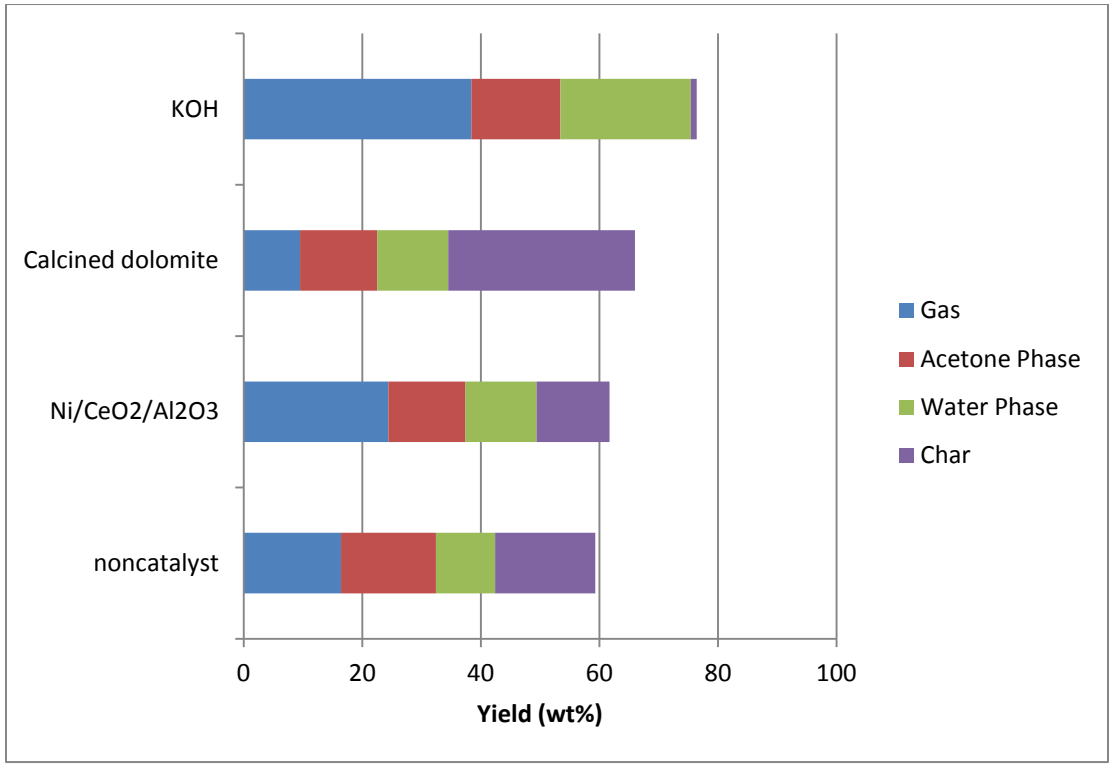

Figure 4.5: Effects of catalysts on product yields (wt%) for 0.65 g cellulose gasification carried out with 4.55 g H_2O and 0.65 g solid catalyst ($Ni/CeO_2/Al_2O_3$ or dolomite) or 0.42 g KOH at 550^oC

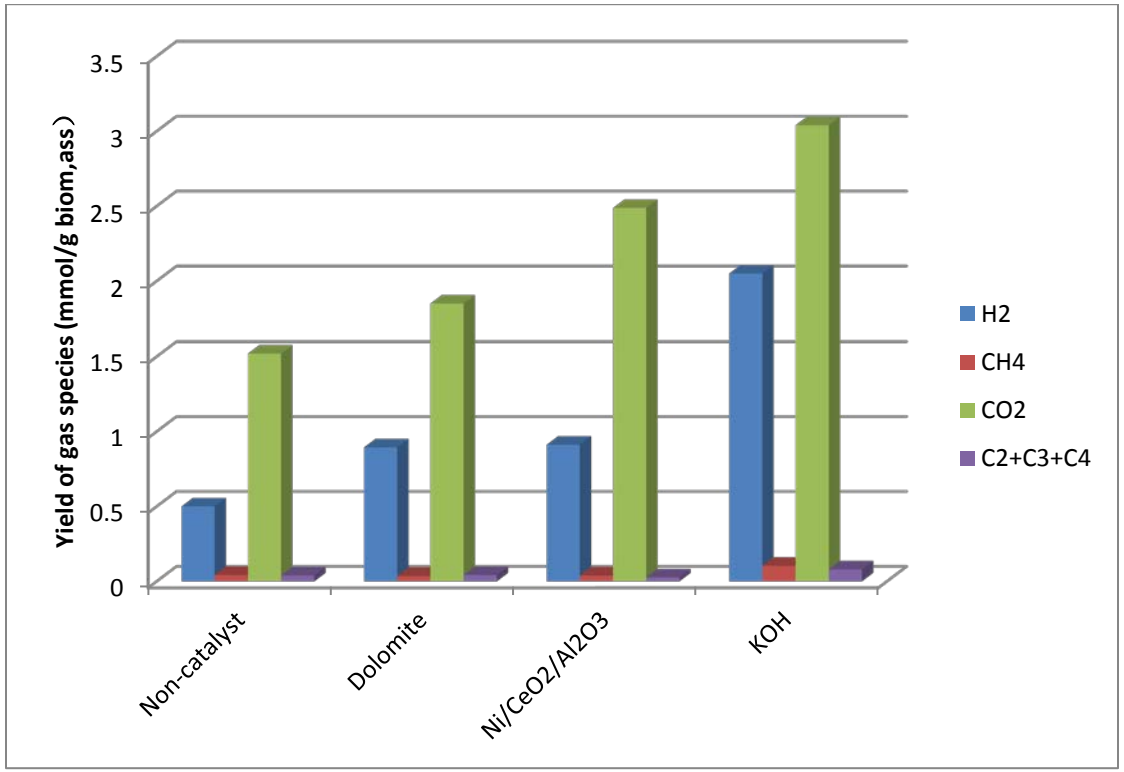

Figure 4.6: Yields of gas species (mmol/g cellulose) for SCW treatment of cellulose (water to biomass ratio of 3:1) for 30 min at a 400^{o}C with various catalysts.

From the results presented in Figure 4.4 and Fig 4.6, $Ni/CeO_2/Al_2O_3$ showed a greater effect on glucose gasification than on cellulose SCWG. This may be due to the complex pathway of cellulose gasification, as cellulose was decomposed to simple sugars and then gasified to fuels. Cellulose is connected via β (1→4)-glycosidic bonds, which allows strong intra- and inter-molecule hydrogen bonds to form, and thus makes cellulose crystalline, and resistant to swelling in water (Peterson *et al*., 2008). The reaction scheme of cellulose gasification is shown in Figure 4.7 (Kruse *et al*. 2004).

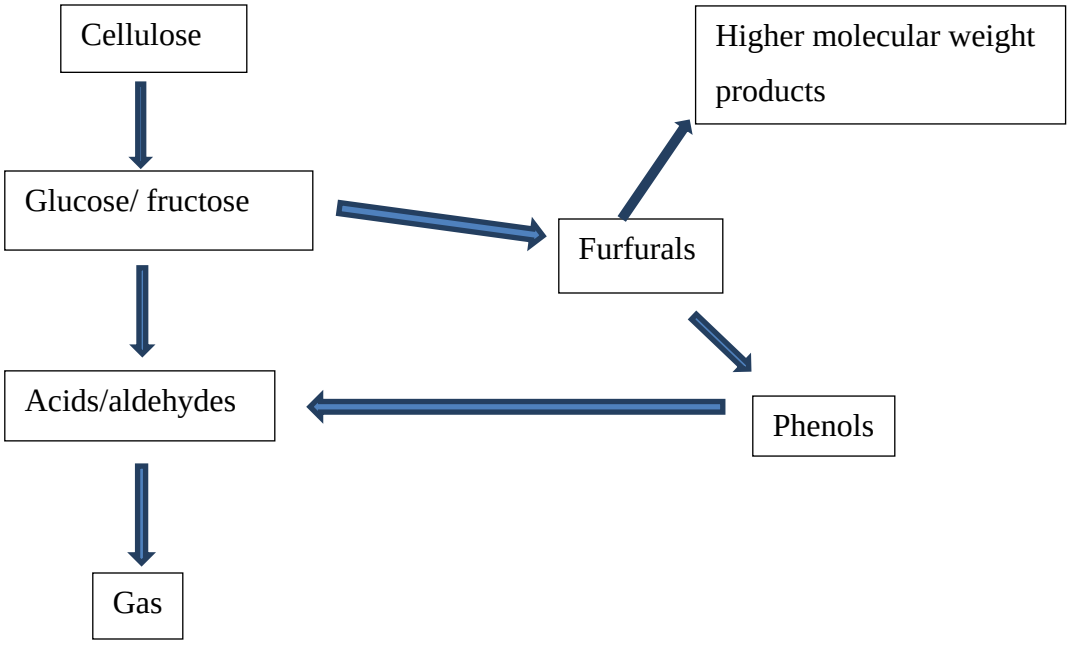

Figure 4.7 Reaction scheme of cellulose SCWG (Kruse *et al*., 2004).

Kruse *et al*., (2004) proposed the mechanism of cellulose gasification in SCW. Cellulose is hydrolyzed to sugar units such as glucose or fructose, and then decomposed to acids and alcohols of 1-3 carbon. Some glucose is degraded to furfurals which are further condensed to phenols and dehydrated to acids. All of these intermediates are highly reactive and readily cracked to gases (Yanik, *et al*., 2007).

4.5.6 Catalytic gasification of pinewood

As a real biomass material, pinewood was gasified in supercritical water using the suitable operating conditions (550^{o}C with a water to biomass ratio of 7:1) obtained from previous runs

and using three catalysts: $Ni/CeO_2/Al_2O_3$, dolomite and KOH. The gas component yields are presented in Table 4.11, together with these for cellulose gasified at the same operating conditions. Figure 4.8 shows the effects of catalysts on product yields (wt%) for 0.65 g pinewood gasification carried out with 4.55 g of H_2O and 0.65 g of solid catalyst ($Ni/CeO_2/Al_2O_3$ or dolomite) or 0.42 g of KOH at 550^oC. As shown in Table 4.11, at the same operating conditions, the gasification of cellulose produced higher yields of H_2 and lower yields of the solid phase.

As shown in Figure 4.8, the mass balance falls in the range of 61-76wt%. From Figure 4.8, the results for the non-catalytic process showed that at 550^oC, about 14% w/w of pinewood was extracted into acetone, while 15% w/w of water soluble product was recovered from the liquid product. 20% w/w gas was formed, while about 19% w/w of products was converted into char.

As shown in Figure 4.8, in the presence of KOH, the gas yield was increased from 20% w/w without catalyst to 25.2% w/w, and solid product formation was reduced from 19% w/w without catalyst to 6% w/w. The gas yield was decreased slightly from 20% w/w without catalyst to 16% w/w using $Ni/CeO_2/Al_2O_3$, while the yield of solid product was reduced from 19% w/w without catalyst to 15% w/w using $Ni/CeO_2/Al_2O_3$. In the meantime, Table 4.11 shows that the presence of $Ni/CeO_2/Al_2O_3$ increased the yield of H_2 from 0.83 mmol/g pinewood without catalyst to 1.3 mmol/g pinewood. As shown in Table 4.11, among all the catalysts, KOH had the best activity for improving H_2 formation, i.e. the H_2 yield increased from 0.83 mmol/g pinewood without catalyst to 5.55 mmol/g pinewood using KOH as catalyst. The presence of $Ni/CeO_2/Al_2O_3$ contributed to a 56.6% increase in H_2 yield.

Calcined dolomite had a quite different effect on pinewood gasification compared with the other two catalysts. As shown in Figure 4.8, the gas yield decreased from 20% w/w without catalyst to 13% w/w using calcined dolomite, while the yield of solid product increased from 19% w/w without catalyst to 36% w/w using calcined dolomite. Table 4.11 shows that the presence of calcined dolomite increased the yield of H_2 from 0.83 mmol/g pinewood without catalyst to 0.99mmol/g pinewood. The difference was mainly caused absorption of CO_2 during biomass gasification by calcined dolomite, which in turn decreased the weight of gas product and increased the yield of solid product.

As shown in Table 4.2, pinewood consists of about 39.0wt% cellulose, 34.0% hemicellulose and 12wt% lignin. These compounds may interact with each other and make the biomass difficult to be gasified. Among three compounds, hemicellulose does not have a crystalline form and is not as resistant as cellulose, thus it is much more susceptible to hydrothermal extraction and hydrolysis. Many researchers have demonstrated that lignin is the most difficult part to be gasified in supercritical water (Guo *et al*., 2010, Calzavara *et al*., 2005, Furusawa *et al*., 2007). Lignin is the most complex compound. It is a three-dimensional, highly branched, polyphenolic substance that consists of an irregular array of variously bonded "hydroxyl-" and "methoxy-" substituted phenylpropane units (Huber and Dumesic, 2006). Lignin is often associated with cellulose and hemicellulose making up lignocellulose (real biomass), which must be broken down to make the cellulose or hemicellulose accessible to hydrolysis (Huber and Dumesic, 2006). During the gasification process, cellulose is hydrolyzed to glucose, hemicelluloses to glucuronic acid and xylose and lignin to phenols. Then glucose is dehydrated to form 5-hydroxymethyl furfural (5-HMF) (Waldner and Vogel. 2005). The phenols can be dehydrated to form aromatics and in turn may by pyrolyzed to coke, while the hydroxylation of phenols leads to polyphenols. Furthermore, phenols are found to be rather inert with respect to gasification. Minowa and Fang (2000) proved the kinetics of decomposition of 5-HMF and polyphenols to low-molecular-weight carboxylic acids, aldehydes, alcohols and ketones at suitable reaction conditions. Thus, these small molecules can by catalyzed to form H_2, CH_4, CO and CO_2. In the meantime, polyphenols can condense to form oligomeric (tar-like substances). This explains the greater yields of solid phase and the smaller yield of H_2 and from pinewood in Table 4.11.

As shown in Table 4.3, pinewood contains some moisture and ash, which could also lead to the lower yield of the gas phase. There is a trace amount of nitrogen and sulfur in pinewood, which may contribute to the deactivation of catalysts.

4.6 Characterizations of liquid/solid products

The elemental compositions (C, H, N and S) of the acetone phase and solid phase products obtained at 500^{o}C from glucose gasification with a residence time of 30 min with and without catalyst are comparatively presented in Table 4.12. In addition, the higher heating values (HHV) for acetone phase and solid phase products are also given. The higher heating value (HHV)

Table 4.11: Effects of catalyst on gas components yields (mmol/g of biomass) for cellulose and pinewood runs at 550^{o}C with a water to biomass ratio of 7:1.

Feedstock	Cellulose				Pinewood			
Catalyst	Non-catalyst	$Ni/CeO_2/Al_2O_3$	Dolomite	KOH	Non-catalyst	$Ni/CeO_2/Al_2O_3$	Dolomite	KOH
H_2	1.16±0.04	1.63±0.05	1.69±0.03	9.09±0.06	0.83±0.01	1.3±0.03	0.99±0.03	5.55±0.05
CH_4	0.82±0.03	1.35±0.03	0.86±0.02	0.65	1.21±0.02	0.87±0.01	0.82±0.03	1.98±0.04
CO_2	2.88±0.05	4.68±0.04	1.35±0.05	6.38±0.05	3.49±0.03	2.92±0.02	2.28±0.02	4.3±0.02
$C_2+C_3+C_4$	0.19	0.23	0.29±0.01	0.22	0.29	0.18	0.3	0.5
LHV (kJ/Nm3)	107	102	166	82.5	122	107	128	132
Solid phase (g)	0.17	0.12	0.32	0.01	0.19	0.15	0.36	0.06

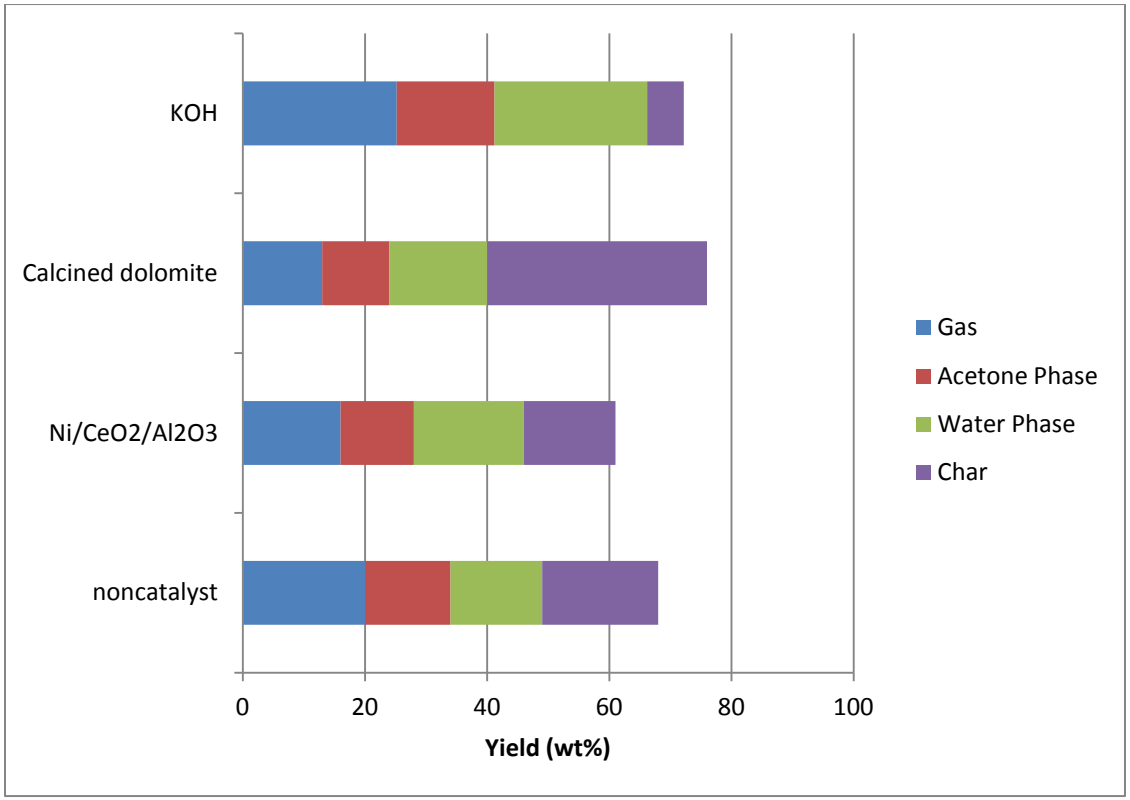

Figure 4.8: Effects of catalysts on product yields (wt%) for 0.65 g pinewood gasification carried out with 4.55 g H_2O and 0.65 g solid catalyst ($Ni/CeO_2/Al_2O_3$ or dolomite) or 0.42 g KOH at 550^oC

refers to the heat released from fuel combustion by a specified quantity (initially at 25°C) with the original and generated water in a condensed state (returned to a temperature of 25°C), which takes into account the latent heat of vaporization of water in the combustion products (Sheng and Azevedo, 2005).

Higher heating value (HHV) by the Dulong formula:

$$HHV\ (MJ/kg) = 0.3383C + 1.422(H - O/8)\ \text{(Yu } et\ al.\text{, 2011).} \qquad (4.3)$$

The results for cellulose gasification are presented in Table 4.13. The solid products may derive from the undecomposed biomass. Aromatic compounds or other unsaturated species can be polymerized to char or tar materials.

From Table 4.12 and Table 4.13, the carbon contents of acetone phase products obtained from runs with catalysts were larger than these for without catalyst. The higher heating value (HHV) of the acetone phase product derived from glucose gasification increased from 29 MJ/kg for runs without catalyst to 33-35 MJ/kg for runs with catalyst. The higher heating value (HHV) of the acetone phase product derived from cellulose gasification increased from 29 MJ/kg for runs without catalyst to 35-36 MJ/kg for catalytic runs. These results suggest that CSCWG is a promising technique to product liquid fuels with greatly increased calorific values. Similar results were reported by Minowa T *et al*.(1998) when treating different biomass feedstocks in hot–compressed water at 300^{o}C. The oil products obtained consisted of 67-75 wt% C, 6.1-8.1 wt% H, 0-2.2 wt% N and 17-24 wt% O, with the gross calorific value falling in the range of 28-33 MJ/kg.

As shown in Table 4.12, the carbon content of acetone phase products derived from glucose increased by about 8-11% when using catalysts in the gasification process. The same trend was seen in Table 4.13 where the presence of catalyst increased the carbon content of the acetone phase by about 11-13%. This means for runs with catalyst, the acetone phase product had a lower oxygen content and thus a greater gross calorific value. Biomass pyrolysis oils generally have a lower calorific value of about 16-19 MJ/kg. Thus, CSCWG is a promising process for producing high quality oils.

It is generally accepted that the biomass fast pyrolysis oils generally consist of 54-58wt% carbon and 35-40wt% oxygen and hence have a much lower calorific value (16 – 19 MJ/kg) (Czernik and Bridgewater, 2004). With respect to the energy content, the heavy oil products (acetone phase) obtained in this work are of a much higher quality than the biomass pyrolysis oils. During pyrolysis, at a high temperatures, the light decomposed fragments from biomass were converted to oil through homogenous reactions, but the high operating temperature favors thermal cracking to form light oils and gases (Xu and Donald, 2008). On the contrary, with the treatment of biomass in supercritical water at a relatively low temperature, the decomposed fragments will repolymerize into oil compounds with larger molecular weights, and thus have a greater heating value.

As shown in Table 4.12 and Table 4.13, compared to treatments without catalyst, the char from the treatments with catalysts had reduced oxygen contents and had greater HHVs. This result may suggest that the catalysts were effective for promoting carbonization of biomass. The LHV of products are also shown in Table 4.12 and Table 4.13. The LHVs were calculated from the HHVs by the following equation:

$$\mathrm{LHV} = \mathrm{HHV} - \mathrm{h} * (w_{water\ out}/\mathrm{w}_{fuel\ in}) \tag{4.4}$$

where h is the latent heat of water at 100^{o}C.

For example: The HHV of glucose is 13.9MJ/kg, the latent of water at 100^{o}C is 2.26 MJ/kg. Assume the weight of glucose was 100kg, and then the weight of water formed was 62.1kg. The LHV of glucose was calculated as:

$$\mathrm{LHV} = \frac{13.9\mathrm{MJ}}{kg\ fuel} - \frac{2.26\mathrm{MJ}}{kg\ water} * \frac{62.1kg\ water}{100kg\ fuel} = 12.5\mathrm{MJ/kg}$$

The chemical composition of the acetone phase, for runs with catalyst at 500^{o}C and a water to biomass ratio of 7:1 was analyzed by GC/MS. The results are shown in Figure 4.9. From Figure 4.9, it is clear that phenols and ketones are the major compounds identified in the acetone phase product (bio-oil). The total amount of detected compound fell in the range of 36-45%. This was because only a portion of the acetone phase product can be detected via GC. As reported by Mohan et al. (2006), bio-oil contains polar, nonvolatile components that are only detectable by

Table 4.12: Elemental analysis results of the acetone phase and solid phase as well as the higher heating value (HHV) for products obtained in the SCW treatment of glucose at water to biomass ratio of 7:1 for 30 min at 500^{o}C

Sample	Elemental analyses (wt%)			HHV (MJ/kg)	LHV (MJ/kg)
	C	H	O[a]		
Glucose	39.99±0.05	6.89±0.05	53.12	13.9	12.5
Acetone phase, non-catalyst	70.91±0.05	6.62±0.04	22.36	29.4	28.1
Acetone phase, Ni/MgO	76.74±0.04	7.28±0.04	15.74	33.5	32.0
Acetone phase, NaOH	79.14±0.05	7.94±0.03	12.82	35.8	34.2
Char, non-catalyst	78.26±0.04	3.70±0.02	17.94	28.6	27.8
Char, Ni/MgO	79.35±0.05	3.11±0.03	17.54	28.1	27.5
Char, NaOH	80.23±0.04	2.95±0.01	16.73	28.4	27.8

[a] By difference and all the samples are dry-ash-free

Table 4.13: Elemental analysis results of the acetone phase and solid phase as well as the higher heating value (HHV) for products obtained in the SCW treatment of cellulose at water to biomass ratio of 7:1 for 30 min at 400^{o}C

Sample	Elemental analyses (wt%)			HHV	LHV
	C	H	O[a]	(MJ/kg)	(MJ/kg)
Cellulose	42.63±0.06	6.61±0.01	50.76	14.8	13.5
Acetone phase, non-catalyst	70.88±0.08	6.48±0.02	22.64	29.2	27.9
Acetone phase, KOH	78.39±0.06	8.48±0.03	13.13	36.2	34.5
Acetone phase, dolomite	79.71±0.05	7.64±0.01	12.65	35.6	34.05
Acetone phase, Ni/CeO_2/Al_2O_3	79.52±0.06	7.32±0.02	13.16	35.0	33.5
Char, non-catalyst	74.07±0.02	3.86±0.01	22.07	26.6	25.8
Char, KOH	82.04±0.03	4.17±0.02	13.79	31.2	30.4
Char, dolomite	79.23±0.04	4.05±0.01	16.72	29.6	28.8
Char, Ni/CeO_2/Al_2O_3	79.56±0.03	3.99±0.02	16.45	29.7	28.9

[a] By difference and all the samples are dry-ash-free

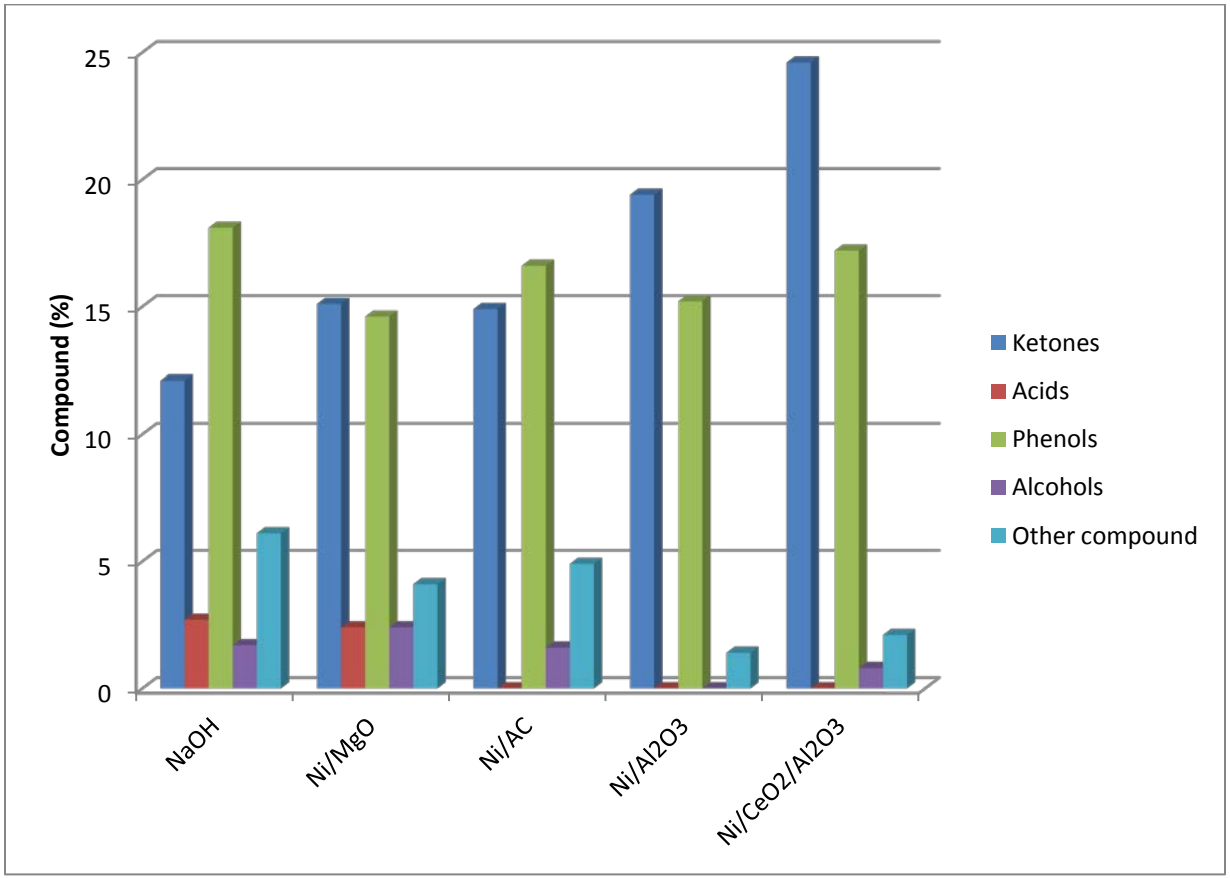

Figure 4.9: GC/MS results for acetone phase products derived from catalystic glucose gasification at 500^{o}C and water to biomass ratio of 7 for 30min.

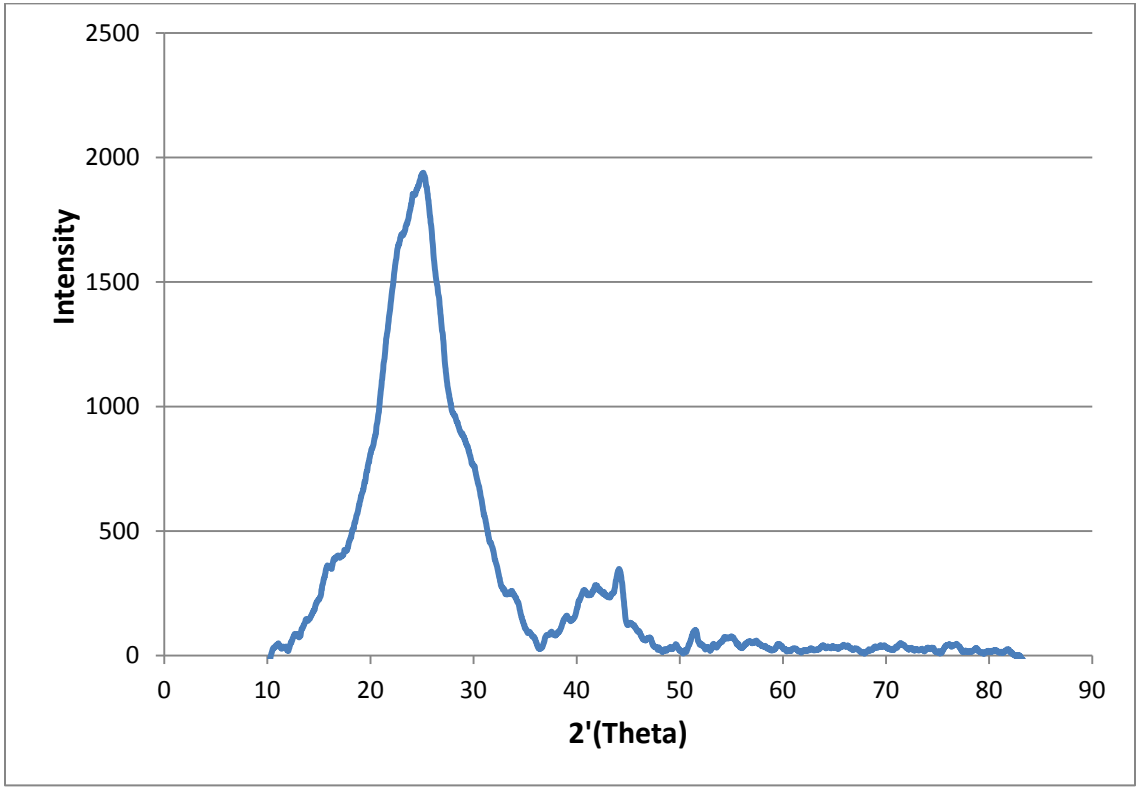

Figure 4.10: X-ray diffraction of solid phase product produced at T=500^{o}C, water to biomass ratio of 3:1, and a residence time of 30 min.

HPLC or GPC analysis. In bio-oil, the volatile compounds can be analyzed by GC-MS, the nonvolatile compounds can be analyzed by HPLC, the functional groups are detectable by fourier transform infrared (FTIR) spectroscopy, the molecular weight distributions can be analyzed by gel permeation spectroscopy (GPC), and types of hydrogens or carbons in specific st ructural groups can be analyzed by nuclear magnetic resonance (NMR) (Mohan D et al., 2006).

Figure 4.10 shows the X-ray diffraction spectrum for the solid phase product produced at 500oC. A small graphite-like structure was found with two peaks at 2θ= 24.6 o and 43.7 o. This indicates an amorphous carbon structure with randomly oriented aromatic carbon sheets (Yu et al., 2011).

4.7 Total mass balance calculation

The total weight balance was calculated for glucose gasification (0.65 g) at 500^{o}C with a water to biomass ratio of 7:1 for 30 min without catalyst. After loading the biomass and water into the reactor, the reactor was weighed (W_0). The reactor was weighed again after releasing the gas product to a gas collection bag after the reaction (W_1). The weight of gas product was calculated according to the results from GC analysis (W_g). The results are shown in Table 4.14.

Mass loss = W_0 **–** (**W_{1+}** W_g) = 102.52 g - (102.00 g + 0.11 g) = 0.41 g

Mass of reactant = 0.65 g glucose + 4.55 g H_2O = 5.2g

Total mass balance = 1- mass loss/mass of reactant = 1- 0.41 g/5.2 g = 92.1%

Table 4.14 Total mass balance

W_0	W_1	W_g	Total mass balance
102.52g	102.00g	0.11g	92.1%

This mass balance data indicated that about 92% of the mass is recovered from this process.

4.8 Carbon balance calculation

The carbon balance was calculated for runs of both glucose and cellulose, and it fell in the range of 85-93%. Table 4.15 shows the mass balance calculation for glucose gasification without catalyst at 500^{o}C with a water to biomass ratio of 7:1 for 30 min and the carbon balance was calculated to be 87.7%. Table 4.16 shows the mass balance calculation for cellulose gasification without catalyst at 400^{o}C with a water to biomass ratio of 7:1 for 30 min, and the carbon balance was calculated to be 88.7%

Table 4.15: Carbon balance calculation for glucose gasification without catalyst at 500^{o}C with a water to biomass ratio of 7:1 for 30 min.

Material	Weight	Carbon content in the compound (wt%)	Carbon weight	Carbon balance
Glucose	1 g	40.0	C_c= 0.400 g	
Solid product	0.21 g	78.3	C_s =0.164 g	41.0%
Water phase	0.091 g	66.5	C_w=0.061 g	15.2%
Acetone phase	0.115 g	70.9	C_a =0.082 g	20.5%
Gas phase			C_g =0.044 g	11.0%
				Total: 87.7%

Table 4.16 Carbon balance calculation for cellulose gasification without catalyst at 400°C with water to biomass ratio of 7:1 for 30 min.

Material	Weight	Carbon content in the compound (wt%)	Carbon weight	Carbon balance
Cellulose	1 g	42.6	C_c= 0.426 g	
Solid product	0.277 g	74.1	C_s =0.205 g	48.1%
Water phase	0.118 g	64.3	C_w=0.076 g	17.8%
Acetone phase	0.082 g	70.88	C_a =0.058 g	13.6%
Gas phase			C_g =0.039 g	9.2%
				Total: 88.7%

4.9 Energy balance calculation

The energy balance for glucose gasification at 500°C and water to biomass ratio of 7:1 without catalyst was calculated. As shown in Table 4.17, the higher heating values (HHVs) of gas species were obtained from http://www.engineeringtoolbox.com/fuels-higher-calorific-values-d_169.html. The energy content of each gas species was calculated and added together to be the HHV of the gas product. One example is given below:

$$Energy\ content\ of\ hydrogen = 141790kJ/kg * 0.77 * 10^{-3}mol * 2 * 10^{-3}kg/mol$$
$$= 0.218kJ$$

In Table 4.17, C_nH_m represents hydrocarbons including ethane, ethylene, propane, propylene, acetylene and I-butane. The higher heating value of propane was used to calculate the approximate heat content in hydrocarbons.

Table 4.17. Calculation for energy content of gas phase

	HHV(kJ/kg)	Amount (mmol)	Molecular weight (g/mol)	Energy (kJ)
Hydrogen	141790	0.77	2	0.218
Methane	55530	0.57	16	0.506
Carbon monoxide	10094	0.52	28	0.147
CnHm	50350	0.12	44	0.266
Total				1.14

Table 4.18 shows the HHVs for liquid and solid products. The HHVs were calculated and listed in Table 4.12. The energy content of each compound was calculated by multipling the HHV with the amount of product recovered from glucose gasification.

Calculation for heating water from 25^{o}C, 10.3MPa to 500^{o}C, 25MPa:

$$Q = (h_f - h_0) * m = \left(\frac{3165.03kJ}{kg} - \frac{114.3kJ}{kg}\right) * 4.55 * 10^{-3}kg = 13.9kJ$$

Table 4.18. Calculation for energy content of liquid phase and solid phase products

	HHV(MJ/kg)	Amount(g)	Energy (kJ)
Liquid (acetone phase + water phase [a])	29.4	0.206	6.06
Char	28.6	0.21	6.01

[a] HHV of water phase was assumed to be the same as that of acetone phase

Where h_f represents the enthalpy of water at the operating conditions (500^{o}C, 25MPa) and h_0 represents the enthalpy of water at initial conditions (25^{o}C, 10.3MPa) obtained from hysys simulation.

Calculation for energy content of feedstock (1g of glucose was gasified and the HHV of glucose was calculated and listed in Table 4.12):

$$Q = HHV * m = \frac{13.9MJ}{kg} * 1 * 10^{-3}kg = 13.9kJ$$

Table 4.19 shows that the liquid and solid products contain 43.6% and 43.2% of the feedstock's energy. By considering heat input during gasification process, ~21.8% of the overall energy is recovered in the liquid products and ~21.6% of the overall energy is recovered in solid products. Total products give an overall energy efficiency of ~48% for glucose gasification. The balance of the energy is attributed to the energy lost in the condensation process and in unaccounted products, which is about 10% of the total feed.

Table 4.19. Energy balance calculation for glucose (water to biomass ratio of 7:1, 500 ^{o}C)

Product [a]	Glucose (13.9kJ)	Glucose + Heat (27.8kJ)
Liquid	43.6%	21.8%
Solid	43.2%	21.6%
Gas	8.2%	4.1%
Total	95%	47.5%

[a] Products are obtained by supercritical water treatment.

5. Summary and Conclusions

5.1 Summary

In this work, glucose, cellulose and pinewood were converted to gas, liquid and solid phase products by SCWG at different operating conditions with and without catalyst.

For non-catalytic runs:

- The products of glucose gasification consisted of approximately 8-17wt% gas, 21-24wt% solid phase, 9-16wt% acetone phase and 8-10wt% water phase. The products from non-catalyst cellulose gasification consisted of approximately 8-17wt% gas, 17-34wt% solid phase, 8-14wt% acetone phase and 8-12wt% water phase.

- As expected, in glucose and cellulose gasification, the gas yield increased with an increase in process temperature while the solid phase yield decreased. For both water to biomass ratios (3:1 and 7:1), the yield of all gas species derived from glucose and cellulose gasification increased with an increase in operating temperature.

- When the temperature was increased from 400 to 500^{o}C for glucose gasification, the CE increased by 78.9% at a 3:1 water to biomass ratio and by 77.4% at a 7:1 water to biomass ratio. For cellulose gasification, the CE increased by 182% at 3:1 water to biomass ratio and by 227% at a 7:1 water to biomass ratio when temperature was increased from 400 to 550^{o}C.

- For glucose and cellulose gasification, the water to biomass ratio had a negligible effect on the yield of C_2+C_3+C_4, and the yield of CH_4 and CO_2 increased slightly with an increase in water to biomass ratio. When the water to biomass ratio increased from 3 to 7, the H_2 yield for glucose gasification was increased by 40% and 33% at 400 and 500^{o}C and the H_2 yield of cellulose gasification was increased by 44%, 11% and 22% at 400, 470 and 550^{o}C, respectively.

For catalytic runs:

- For glucose gasification, NaOH had the best activity for improving H_2 formation, as the H_2 yield increased by 135% with NaOH catalyst at 500^{o}C. The yield of H_2 was increased by 60% with $Ni/CeO_2/Al_2O_3$ and by 52% with Ni/Al_2O_3. The results indicate that the presence of Ce improved the activity of Ni/Al_2O_3.

- The mass balance obtained from glucose gasification with catalyst was in the range of 55-74%. The unaccounted portion of the original material may be due largely to water loss and evaporation of products during the water removal process used in the recovering of the water phase product.

- For cellulose gasification, KOH had the best activity for improving H_2 formation, as the H_2 yield increased by 194% with the use of the KOH catalyst. The presence of $Ni/CeO_2/Al_2O_3$ contributed to a 30.7% increase in H_2 yield, followed by a 28.3% increase with dolomite.

- LHVs of gas products derived from glucose and cellulose with catalysts were calculated to be in the range of 60.6-143 kJ/Nm^3 and 74.6-198 kJ/Nm^3, respectively.

- The higher heating value (HHV) of the acetone phase product derived from glucose gasification increased from 29 MJ/kg without catalyst to 33-35 MJ/kg with catalyst. The higher heating value (HHV) of the acetone phase product derived from cellulose gasification increased from 29 MJ/kg without catalyst to 35-36 MJ/kg with catalyst.

- At the same operating conditions with the same catalysts, the gasification of cellulose exhibited higher yields of H_2 and lower yields of the solid phase product than did gasification of pinewood.

- By comparing the results from glucose, cellulose and pinewood gasification, it was proven that lignin is the most difficult material to be gasified and the alkali catalysts had the best effect on promoting the yield of H_2 during biomass gasification.

For the catalysts study

- When AC and Ni/AC were used at the same operating conditions, the results showed that hydrogen production increased by 6.9% with activated carbon and 36.9% with Ni/AC, while the carbon dioxide yield increased by 94.2% with activated carbon and 124.2% with Ni/AC. The run with activated carbon produced a higher yield of the solid phase product at 25.4wt% compared with 20wt% using Ni/AC.

- When KOH and NaOH were used at the same operating conditions, the hydrogen yield increased by 312% with KOH and 180% with NaOH. The run with KOH had a 5.4wt% higher yield of char and a 4.6wt% lower yield of the acetone phase product compared to the run with NaOH.

- A small amount of H_2 was formed with Ni-based catalyst/dolomite and water. This was caused by oxidization of Ni in supercritical water. Also, there was some CO_2 formed during the Ni/AC and water run; this was due to the reaction between C and water.

- Dolomite and olivine were used as catalysts for cellulose gasification at 400 ^oC with a water to biomass ratio at 3:1. The H_2 yields were 0.916 and 0.824 mmol/g cellulose, while the tar yields were 0.17 and 0.19 g in the presence of dolomite and olivine, respectively.

For products characterization:

- Phenols and ketones were the major compounds identified in the acetone phase product.

- The solid product had an amorphous carbon structure with randomly oriented aromatic carbon sheets

5.2 Conclusions

- During gasification of biomass such as pinewood, the major gaseous products are H_2, CO, CO_2 and CH_4 whereas the acetone phase product mainly contains phenols and ketones.

- Higher temperature and 7:1 water to biomass ratio contributed to higher yield of H_2 and suppressed the formation of char.

- Alkali catalysts are more effective than Ni-based catalysts and calcined dolomite.

- Calcined dolomite is a promising catalyst on promoting H_2 yield from SCWG of biomass.

5.3 Recommendations

- From this project, it was demonstrated that alkali catalysts were quite effective for improving H_2 production and suppressing the formation of char or tar, but they may cause corrosion problems. Thus, it is recommended to study the corrosive effect of alkali catalysts on reactor walls.

- The reactor used in this project was made from 3/8-inch diameter stainless steel tubing; the small volume limited the amount of biomass involved in each run. A larger reactor would make it easier to collect products and thus improve the mass balance.
- It is recommended to utilize a more powerful furnace to provide a higher heating rate for the reactor. This would increase the carbon efficiency of biomass gasification.

- More water to biomass ratios should be studied to find the exact trend of its effect on biomass gasification. Also, a systematic process optimization study may be carried out.

- A new catalyst is recommended for future studies: Ni/dolomite. As both Ni-based catalyst and dolomite can improve H_2 yields and suppress char formation, Ni/dolomite might have a better effect on biomass gasification.

- Lignin gasification with SCW may be considered to obtain both gaseous fuel and liquid chemicals.

- A continuous system could be used to study this process to use feedstock more efficiently.

References

Antal M. J., S Allen, D Schulman, X Xu, RJ Divilio, “Biomass gasification in supercritical water,” Industrial & Engineering Chemistry Research. 39, 4040-4053(2000).

Aymonier C, A. Loppinet-Serani, H. Revero’n, Y. Garrabos and F. Cansell, “Review of supercritical fluids in inorganic materials science,” J Supercrit Fluids 38, 242–251(2006).

Azargohar R. and A. K. Dalai, “Production of activated carbon from luscar char: Experimental and modeling studies,” Microporous and Mesoporous Materials. 85, 219-225(2005).

Basu P., V. Mettanant, “Biomass gasification in supercritical water-A review,” International Journal of Chemical Reactor Engineering.7, 1-63(2009).

Boukis N., V. Diem, W. Habicht, E. Dinjus, “Methanol reforming in supercritical water,” Industrial & Engineering Chemistry Research. 42, 728-735(2003).

Botchwey C, Syntheses, characterization and kinetics of nicke-tungsten nitride catalysts for hydrotreating of gas oil. Unpublished PhD thesis, University of Saskatchewan. (2010)

Byrd A. J., K. K. Pant, R. B. Gupta, “Hydrogen production from glucose using Ru/Al_2O_3 catalyst in supercritical water,” Industrial & Engineering Chemistry Research. 46, 3574 – 3579(2007).

Calzavara Y., C. Joussot-Dubien, G. Boissonnet, S. Sarrade, “Evaluation of biomass gasification in supercritical water process for hydrogen production,” Energy Conversion and Management. 46, 615 – 631(2005).

Corella J., J.M. Toledo and R. Padilla, “Olivine or dolomite as In-Bed additive in biomass gasification with air in a fluidized bed: which is better,” Energy & Fuels. 18, 713-720(2004).

Corbo P., F. Migliardini, “Natural gas and biofuel as feedstock for hydrogen production on Ni catalysts,” Journal of Natural Gas Chemistry. 18, 9-14(2009).

Czernik C., AV. Brigewater, “Overview of applications of biomass fast pyrolysis oil,” Energy Fuels. 18, 590-598(2004).

Davda R.R., J. W. Shabaker, G. W. Huber, R. D. Cortright, J. A., Dumesic, “Aqueous-phase reforming of ethylene glycol on silica-supported metal catalysts,” Applied Catalysis B Environmental. 43, 13 – 26(2003).

Demirbas A., “Hydrogen-rich gas from fruit shells via supercritical water extraction,” International Journal of Hydrogen Energy. 29, 1237-1243(2004).

Devi L., K. J. Ptasinskia, F. J. J. G. Janssena, S. V. B. V. Paasenb, P. C. A. Bergmanb, J. H. A. Kiel, “Catalytic decomposition of biomass tars: use of dolomite and untreated olivine,” Renewable Energy. 30, 565-578(2005).

Elliott D. C., “Catalytic hydrothermal gasification of biomass,” Biofuels Bioproducts and Biorefining. 2, 254-265(2008).

Fang Z., T. Minowa, R. L. Smith, Jr. T. Ogi, J.A. Kozinski. “Liquefaction and Gasification of Cellulose with Na_2CO_3 and Ni in Subcritical Water at 350° C,” Ind.Eng.Chem. 42, 2454-2463(2004).

Furusawa T., T. Sato, M. Saito, Y. Ishiyama , M. Sato, N. Itoh, N. Suzuki, “The evaluation of the stability of Ni/MgO catalysts for the gasification of lignin in supercritical water,” Applied Catalysis General. 327, 300 – 310(2007).

Guo L. J., Y. J. Lu, X. M. Zhang, C. M. Ji, Y. Guan and A. X. Pei, “Hydrogen production by biomass gasification in supercritical water: a systematic experimental and analytical study,” Catalysis Today. 129, 275-286(2007).

Guo Y., S. Z. Wang, D. H. Xu, Y. M. Gong, H. H. Ma, X. Y. Tang, “Review of catalytic supercritical water gasification for hydrogen production from biomass,” Renewable and Sustainable Energy Reviews. 14, 334-343(2010).

Hao X. H., L. J. Guo, X. Mao, X. M. Zhang and X. J. Chen, “Hydrogen production from glucose used as a model compound of biomass gasified in supercritical water,” International Journal of Hydrogen Energy. 28, 55-64(2003).

Higman C. and M. V. D. Burgt, Gasification. Gulf Professional Publishing (2003).

Hu G., S. Xu, S Li, C. Xiao, S. Liu, “Steam gasification of apricot stones with olivine and dolomite as downstream catalysts,” Fuel Process Technology. 87, 375-382(2006).

Huber G. W., J. A. Dumesic, “An overview of aqueous-phase catalytic processes for production of hydrogen and alkanes in a biorefinery,” Catalysis Today. 111, 119-132 (2006).

Ikushima Y., K. Hatakeda, O., Sato, T., Yokoyama, M., Arai, “Acceleration of synthetic organic reactions using supercritical water: noncatalytic Beckmann and pinacol rearrangements,” Journal of the American Chemical Society. 122, 1908 – 1918(2000).

Kroschwitz J. I., M. Howe-Grant, D. F. Othmer, R. E. Kirk, “Encyclopedia of chemical technology,” New York: Wiley (1991).

Kruse A., A. Krupka, V. Schwarzkopf, C. Gamard, T. Henningsen, “Influence of proteins on the hydrothermal gasification and liquefaction of biomass,” Industrial & Engineering Chemistry Research 44, 3013 – 3020(2005).

Kruse A., D. Meier, P. Rimbrecht, M. Schacht, “Gasification of pyrocatechol in supercritical water in the presence of potassium hydroxide,” Industrial & Engineering Chemistry Research. 39, 4842 – 4887(2000).

Kruse A., T. Henningsen, A Sinag, J. Pfeiffer, “Biomass gasification in supercritical water: Influence of the dry matter content and the formation of phenols,” Ind. Eng. Chem. Res. 42, 3711-3717(2003).

Lee In-Gu, “Effect of metal addition to Ni/activated charcoal catalyst on gasification of glucose in supercritical water,” International Journal of Hydrogen Energy. 36, 8869-8877(2011).

Lee In-Gu, Mi-Sun Kim, and Son-Ki Ihm, “Gasification of glucose in supercritical water,” Industrial & Engineering Chemistry Research. 41, 1182-1188(2002).

Lee In-Gu, Son-Ki Ihm, “Catalytic gasification of glucose over Ni/activated charcoal in supercritical water,” American Chemical Society Journals. 48, 1435–1442(2009).

Letellier S., F. Marias, P. Cezac, J.P. Serin, “Gasification of aqueous biomass in supercritical water: A thermodynamic equilibrium analysis,” The Journal of Supercritical Fluids. 51, 353-361(2010).

Loppinet-Serani A., C. Aymonier, F. Cansell, “Supercritical water for environmental technologies,” J Chem Technol Biotechnol. 85, 583-589(2010).

Lu Y. J., L. J. Guo, C. M. Ji, X. M. Zhang, X. H. Hao, Q. H.Yan, “Hydrogen production by biomass gasification in supercritical water: A parametric study,” International Journal of Hydrogen Energy. 31, 822-831(2006).

Lv P.M., Z. H. Xiong, J Chang, C.Z. Wu, Y. Chen, J.X. Zhu, “An experimental study on biomass air-steam gasification in a fluidized bed,” Bioresource Technology. 95, 95-101(2004).

Matsumura Y., K. Nagata, Y. Kikuchi, “Effect of heating rate on tarry material production in supercritical water gasification,” Science in Thermal and Chemical Biomass Conversion. 2, 991-1000(2006).

Matsumura Y., T. Minowa, B. Potic, S. R. A. Kersten, W. Prins, W. P. M. V. Swaaij, B. V. D. Beld, D. C. Elliott., G. G. Neuenschwander, A. Kruse and M. J. Antal, “Biomass gasification in near- and super-critical water: status and prospects,” Biomass and Bioenergy. 29, 269-292(2005).

Matsumura Y., X. Xu, Jr. Antal, “Gasification characteristics of an activated carbon in supercritical water,” Carbon. 35, 819-824(1997).

Minowa T., T. Kondo, ST. Sudirjo, “Thermochemical liquefaction of Indonesia biomass residues,” Biomass Bioenergy. 14, 517-524(1998).

Minowa T., Z. Fang, “Hydrogen production from biomass by low temperature catalytic gasification,” Prog. Thermochem. Biomass conversion. A.V. Brigdgwater, Ed. 2000, 396

Mohan D., C.U. Pittman Jr., P. H. Steele, “Pyrolysis of wood/biomass for bio-oil: a critical review,” Energy& Fuel. 20, 848-849(2006).

Muangrat R., J. A. Onwudili, P. T. Williams, “Influence of NaOH, Ni/Al_2O_3 and Ni/SiO_2 catalysts on hydrogen production from the subcritical water gasification of model food waste compounds,” Applied Catalysis B: Environmental. 100, 143-156(2010).

Naik S. N., V. V. Goud, P. K. Rout, K. Jacobson, A. K. Dalai, “Characterization of Canadian biomass for alternative renewable biofuel,” Renewable Energy. 35, 1624-1631(2010).

Onwudili, J. A., P. T. Williams, “Role of sodium hydroxide in the production of hydrogen gas from the hydrothermal gasification of biomass,” International Journal of Hydrogen energy. 34, 5645-5656(2009).

Osada M., N. Hiyoshi, O. Sato, K. Arai, M. Shirai, “Effect of sulfur on catalytic gasification of lignin in supercritical water,” Energy & Fuels. 21, 1400 – 1405(2007).

Park K. C., H. Tomiyasu, “Gasification reaction of organic compounds catalyzed by RuO2 in supercritical water,” Chemical Communications (Cambridge United Kingdom). 6, 694 – 695(2003).

Penninger J. M. L., M. Rep, “Reforming of aqueous wood pyrolysis condensate in supercritical water,” International Journal of Hydrogen Energy. 31, 1597-1606(2006).

Peterson A. A., F. Vogel, R. P. Lachance, M. Fröling, M. J. Antal, J. W. Tester, “Thermochemical biofuel production in hydrothermal media: A review of sub- and supercritical water technologies,” Energy&Environmental Science. 1, 32-65(2008).

Qu Y., X. Wei, C. Zhong, “Experimental study on the direct liquefaction of Canninghamia lanceolata in water,” Energy. 28, 597-606(2003).
Schuster G., G. LoVer, K. Weigl, H. Hofnauer, “Biomass steam gasification—an extensive parametric modeling study,” Bioresource Technology. 77, 71–79(2001).

Rezaiyan J., N. P. Cheremisinoff, “Gasification technologies: A primer for engineers and scientists,” Taylor & Francis (2005)

Sánchez-Sánchez M. C., R.M. Navarro, J.L.G. Fierro, “Ethanol steam reforming over Ni/M_xO_y Al_2O_3(M=Ce, La, Zr and Mg) catalysts: Influence of support on the hydrogen production,” International Journal of Hydrogen Energy 32, 1462-1471(2007).

Sato T., M. Osada, M. Watanabe, M. Shirai, K. Arai, “Gasification of alkylphenols with supported noble metal catalysts in supercritical water,” Industrial & Engineering Chemistry Research. 42, 4277 – 4282(2003).

Sato T., T. Furusawa, Y. Ishiyama, H. Suigo, Y. Miura, M. Sato, N. Suzuki, N. Itoh, “Effect of water density on the gasification of lignin with magnesium oxide supported nickel catalysts in supercritical water,” Ind. Eng. Chem. Res. 45, 615-622(2006).

Satterfield, C. “Heterogeneous Catalysis in Industrial Practice” 2nd Ed. McGraw- Hill (1991)

Schacht C., C. Zetzl, G. Brunner, “From plant materials to ethanol by means of supercritical fluid technology,” Journal of Supercritical Fluids. 46, 299-321(2008).

Sheng C., J. L. T. Azevedo, “Estimating the higher heating value of biomass fuels from basic analysis data,” Biomass&Bioenergy. 28, 499-507(2005).

Sinag A., A. Kruse, J. Rathert, “Influence of the heating rate and type of catalyst on the formation of key intermediates and on the generation of gases during hydropyrolysis of glucose in supercritical water in a batch reactor,” Ind. Eng. Chem. Res. 43, 502-508(2004).

Tang H., K. Kitagawa, “Supercritical water gasification of biomass: thermodynamic analysis with direct Gibbs free energy minimization,” Chemical Engineering Journal. 106, 261 – 267(2005).

Vogel F., M. H. Waldner, “Catalytic hydrothermal gasification of woody biomass at high feed concentration,” Science in Thermal and Chemical Biomass Conversion. 2, 1001-1012(2006).

Waldner M. H., F. Vogel, “Renewable production of methane from wood biomass by catalytic hydrothermal gasification,” Ind. Eng. Chem. Res. 44, 4543-4551(2005).

Wang J., T. Takarada, “Role of calcium hydroxide in supercritical water-gasification of low rank coke,” Energy& Fuels. 15, 356-362(2001).

Watanabe M., H. Inomata, K. Arai, “Catalytic hydrogen generation from biomass (glucose and cellulose) with ZrO_2 in supercritical water,” Biomass Bioenergy. 14, 405–410(2002).

Watanabe M., M. Osada, H. Inomata, K. Arai, A. Kruse, “Acidity and basicity of metal oxide catalysts for formaldehyde reaction in supercritical water at 673 K,” Applied Catalysis A General. 245, 333 – 341(2003).

Weingartner H., E. U. Franck, “Supercritical water as a solvent,” Chem. Int. Ed. 44, 2672-2692(2005).

Williams P. T., J. Onwudili, “Composition of products from the supercritical water gasification for glucose: A model biomass compound,” Industrial and Engineering Chemistry research. 44, 8739-8749(2005).

Xu C., J. Donald, “Upgrading peat to gas and liquid fuels in supercritical water with catalysts,” Fuel. 102, 16-25(2012).

Xu C., N. Lad, “Production of heavy oils with high caloric values by direct-liquefaction of woody biomass in sub-/near-critical water,” Energy Fuels. 22, 635-642(2008).

Xu C., T. Etcheverry, “Effect of iron-based catalysts on hydro-liquefaction of woody biomass in supercritical ethanol,” Fuel. 87, 335-345(2008).

Yanik J., S. Ebale, A. Kruse, M. Saglam, M. Yuksel, “Biomass gasification in supercritical water,” International Journal of Hydrogen Energy. 33, 4520 – 4526(2008).

Yanik J., S. Ebale, A. Kruse, M. Saglam, M. Yüksel, “Biomass gasification in supercritical water: Part 1. Effect of the nature of biomass,” Fuel. 86, 2410-2415(2007).

Yoshida T., Y. Matsumura, “Gasification of cellulose, xylan, and lignin mixtures in supercritical water,” Industrial and Engineering Chemistry Research. 40, 5469-5474(2001).

Yu D., M. Aihara, M. J. Antal Jr., “Hydrogen production by steam reforming glucose in supercritical water,” Energy&Fuel. 7, 574-577(1993).

Yu J., P. E. Savage, “Decomposition of formic acid under hydrothermal conditions,” Ind. Eng, Chem, Res. 37, 2-10(1998).

Yu J. T., A. M. Dehkhoda, and N. Ellis, “Development of biochar-based catalyst for transesterification of canola oil,” Energy&Fules. 25, 337-344(2011).

Yu Y., X. Lou and H. Wu, “Some recent advances in hydrolysis of biomass in hot-compressed water and its comparisons with other hydrolysis methods,” Energy & Fuels. 22, 46-60(2008).

Kruse A. “Supercritical water gasification,” Biofuel, Bioproducts and Biorefining. 5, 415-437(2008).

Appendix A

Equations

A-1 Catalyst Preparation Calculations

A-1.1 Calculation for amounts of precursors in catalyst

For a given catalyst composition X (wt%), the amount of precursor Y (wt) required for synthesis is given by the relation

$$Y = \frac{X * M_C * MM * Z}{M_A * 100} \quad \text{(A.1)}$$

Mc - The total amount of catalyst to be synthesized

MM - The molecular weight of the precursor

Z - the purity of the precursor

M_A - the atomic weight.

For instance, for preparation of 5g 10wt% Ni/Al_2O_3 catalyst, the precursors and support needed are calculated in the following equation:

1. For Ni, $Ni(NO_3)_2 \cdot 6H_2O = \frac{10*5*290.81*97\%}{58.69*100} = 2.40g$

2. The amount Al_2O_3 required is given as,

Composition (%) x Weight of Catalyst Required.

i.e. Amount of Al_2O_3 = 0.9 * 5 = 4.5 g

3. The approximate amount of water required for impregnation is a measure of the alumina pore volume and was given by the relation,

1.4 * Weight of Al_2O_3 * Pore Volume

= 1.4 * 4.5 * 0.62 = 3.91 cm^3

The information about precursor is listed in Table A.1 and the recipe of all catalysts was presented in Table A.2. For preparation of Ni/MgO, because the negligible pore volume of MgO,

the volume of water needed was assumed to be the same as that for Ni/AC. For preparation of $Ni/CeO_2/Al_2O_3$, the recipe was a little more complex as the atomic ratio of Ni/Ce is 0.035. When treating 5g of Al_2O_3, 4.89g $Ni(NO_3)_2{\cdot}6H_2O$ and 1.22g $CeCl_3{\cdot}6H_2O$ are needed as precursors together with 4.34cm^3 of water as solvent. Table A.3 shows the surface area and pore volume of catalyst support.

Table A.1: Precursor used for catalyst preparation.

Element	Precursor	Molecular Weight (g)	Atomic Wt Precursor (g)	Percentage Purity (%)
Ni	$Ni(NO_3)_2{\cdot}6H_2O$	290.81	58.69	97
Ce	$CeCl_3{\cdot}6H_2O$	354.47	140.12	97

Table A.2: Recipe of catalyst (for 5g catalyst)

Catalysts	Weight of $Ni(NO_3)_2{\cdot}6H_2O$ (g)	Volume of Water (cm^3)	Weight of Support (g)
Ni/Al_2O_3	2.40	3.91	4.5
Ni/AC	2.40	1.91	4.5
Ni/MgO	2.40	1.91	4.5

Table A.3: Characterization results of catalyst support

Supports	Surface Area	Total Pore Volume
Al_2O_3	220.8	0.62
AC	502.0	0.30
MgO	4.7	<0.001

A-2 Calculations for Gas Products

A-2.1 Calculation for reaction part's volume

The schematic of the reaction set-up is shown in Figure A.1 The part before Valve 3 is the section for reaction to occur (Figure A.1). The reactor was made from 316 stainless steel tubing with an O.D of 0.95 cm (3/8 inch) and a wall thickness of 0.17cm (0.065 inch) obtained from Swagelok. Before the Valve 3, there are some other parts: a SS-600-C cap, a SS-600-3-5-4 reducing union, a SS-400-R-6 reducer, a SS-100-R-4BT reducer, and a SS-4TF filter, a SS-400-4 union, a SS-4R3A relief valve, a PGI-63C-PG5000-LAQX gauge and three 1.8inch long 1/4 inch tubing.

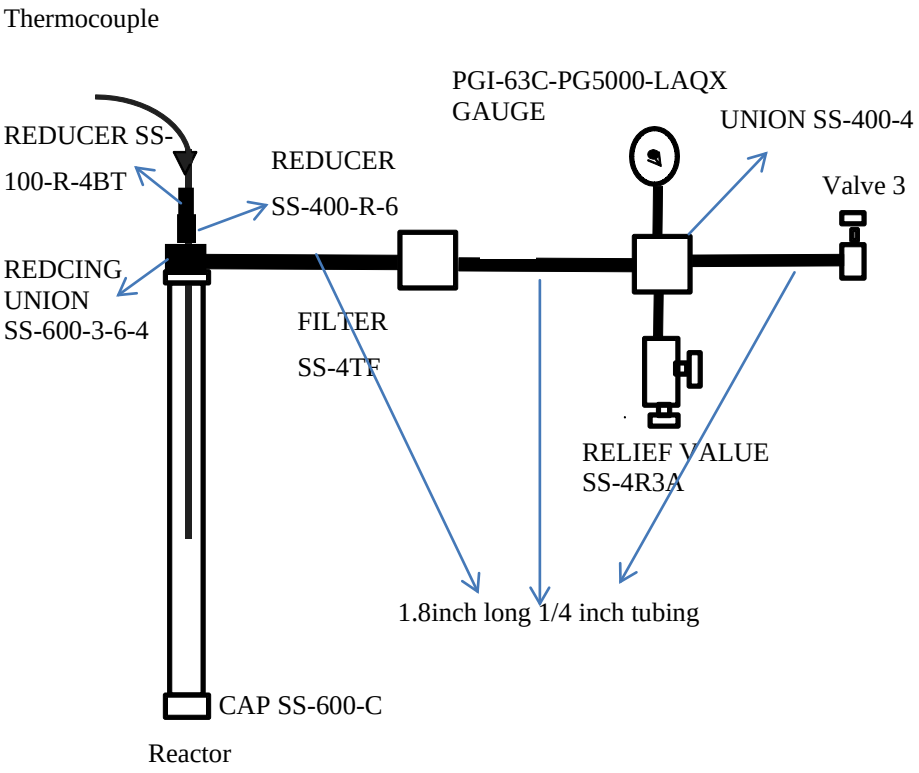

Figure A.1 Reaction part of the experimental set-up.

All the parts were obtained from Swagelok, by checking the dimensions of these parts on Swagelok website, the total volume before Valve 3 was calculated to be 10.75 cm^3.

A-2.2 Calculation for standard gas (nitrogen)

Before each run, the reaction part was purged with nitrogen to get a certain pressure. Nitrogen was used to provide an initial pressure which would help the system reach supercritical conditions at operating temperatures. Furthermore, nitrogen was used as a standard gas for calculation of gas products.

The mole amount of nitrogen was calculated by Ideal Gas Law Equation listed below:

$$PV = nRT \Longrightarrow \quad n = \frac{PV}{RT}$$

P - The pressure of N_2

V - The volume of reaction part

R - 0.082$\frac{atm*L}{mol*K}$

T - The temperature

For instance, glucose gasification at 400^{o}C with water to biomass ratio of 3 has an initial pressure of 2170psi (N_2).

The pressure of N_2=2170psi=147.66atm

The temperature of N_2= room temperature=20^{o}C=293K

The volume of N_2= 10.75 cm^3=0.01075L

$$n = \frac{PV}{RT} = \frac{147.66atm*0.01076L}{0.082\frac{atm*L}{mol*K}*293K} = 0.0661\text{mol} \quad (A.2)$$

A-2.3 Calculation for gas product species

The calculation of gas species was presented in Table A.4. The second column shows the original results from GC analysis and the third column shows the results after normalization. The mole amount of gas species was listed in the last column and calculated according to the following equation:

$$n_i = n_{N_2*}\frac{C_i}{C_{N_2}}$$

n_i - The mole amount of gas species

n_{N_2} - The mole amount of N_2 (has been calculated from equation A.2)

C_i - The normalized N_2 concentration

C_{N_2} - The normalized gas species concentration

Table A.4 Calculation of gas species for glucose gasification at 400^{o}C with water to biomass ratio of 3

Gas species	Concentration from GC analysis (%)	Normalized concentration (%)	Mole amount of gas species (mmol/g of glucose)
H_2	7.77E-01	7.54E-01	8.03E-01
Methane	5.17E-02	5.02E-02	5.30E-02
Ethane	1.46E-02	1.42E-02	1.48E-02
Ethylene	4.68E-03	4.54E-03	4.75E-03
Propane	4.68E-03	4.54E-03	4.62E-03
Propylene	1.38E-02	1.34E-02	1.36E-02
CO_2	2.33E+00	2.26E+00	2.39E+00
Acetylene	0.00E+00	0.00E+00	0.00E+00
I-butane	1.01E-03	9.77E-04	9.01E-05
O_2	5.85E-01	5.68E-01	5.16E-02
N_2	9.93E+01	9.63E+01	1.02E+02
CO	0.00E+00	0.00E+00	0.00E+00
Total	1.03E+02	1.00E+02	

Appendix B

Experimental Data

B-1 Results from Glucose Gasification Data Collection

Table B.1 Sample data collection, for glucose gasification without catalyst

Operating temperature and water to biomass ratio	H_2 (mmol/g of cellulose)	CH_4 (mmol/g of cellulose)	CO_2 (mmol/g of cellulose)	CO (mmol/g of cellulose)	$C_2+C_3+C_4$ (mmol/g of cellulose)	Gas product (g/g of cellulose)	Solid product (g/g of cellulose)
400^{o}C (3:1)	0.52±0.02	0.04	1.84±0.06	0	0.09	0.083±0.002	0.24±0.001
500^{o}C (3:1)	0.58±0.02	0.52	2.21±0.11	0.47±0.01	0.11	0.132±0.003	0.23
400^{o}C (7:1)	0.73	0.07	1.87±0.08	0	0.10	0.112±0.002	0.22
500^{o}C (7:1)	0.77±0.02	0.57±0.02	2.33±0.10	0.52±0.01	0.12	0.164±0.003	0.21±0.001

Table B.2 Sample data collection, for glucose gasification with Ni/Al_2O_3

Operating temperature and water to biomass ratio	H_2 (mmol/g of cellulose)	CH_4 (mmol/g of cellulose)	CO_2 (mmol/g of cellulose)	$C_2+C_3+C_4$ (mmol/g of cellulose)	Gas product (g/g of cellulose)	Solid product (g/g of cellulose)
400^{o}C (3:1)	0.80	0.05	2.39±0.05	0.04	0.126±0.004	0.19
500^{o}C (3:1)	0.91±0.02	0.52±0.01	2.94±0.03	0.18	0.169±0.005	0.14
400^{o}C (7:1)	0.82±0.01	0.15	1.78±0.13	0.09	0.120±0.003	0.15±0.003
500^{o}C (7:1)	0.93±0.02	0.49±0.02	3.36±0.10	0.17	0.176±0.005	0.11±0.001

Table B.3 Sample data collection, for glucose gasification with $Ni/CeO_2/Al_2O_3$

Operating temperature and water to biomass ratio	H_2 (mmol/g of cellulose)	CH_4 (mmol/g of cellulose)	CO_2 (mmol/g of cellulose)	$C_2+C_3+C_4$ (mmol/g of cellulose)	Gas product (g/g of cellulose)	Solid product (g/g of cellulose)
400^{o}C (3:1)	0.83	0.09	2.68±0.07	0.04	0.143±0.002	0.22±0.003
500^{o}C (3:1)	0.91±0.02	0.55±0.02	3.21±0.10	0.16	0.167±0.005	0.17±0.001
400^{o}C (7:1)	0.87	0.06	2.19±0.08	0.03	0.107±0.003	0.14
500^{o}C (7:1)	0.98±0.02	0.93±0.02	3.70±0.05	0.24	0.197±0.003	0.12±0.001

Table B.4 Sample data collection, for glucose gasification with Ni/AC

Operating temperature and water to biomass ratio	H_2 (mmol/g of cellulose)	CH_4 (mmol/g of cellulose)	CO_2 (mmol/g of cellulose)	$C_2+C_3+C_4$ (mmol/g of cellulose)	Gas product (g/g of cellulose)	Solid product (g/g of cellulose)
400^{o}C (3:1)	0.94±0.01	0.13	3.35±0.07	0.08	0.174±0.006	0.28±0.002
500^{o}C (3:1)	0.95±0.03	0.61±0.001	3.80±0.12	0.22	0.216±0.009	0.25
400^{o}C (7:1)	0.98±0.01	0.08	3.48±0.11	0.05	0.159±0.004	0.20±0.001
500^{o}C (7:1)	1.05±0.02	0.35±0.02	5.00±0.05	0.12	0.260±0.003	0.18±0.001

Table B.5 Sample data collection, for glucose gasification with Ni/MgO

Operating temperature and water to biomass ratio	H_2 (mmol/g of cellulose)	CH_4 (mmol/g of cellulose)	CO_2 (mmol/g of cellulose)	$C_2+C_3+C_4$ (mmol/g of cellulose)	Gas product (g/g of cellulose)	Solid product (g/g of cellulose)
400^{o}C (3:1)	0.84	0.08	3.21±0.10	0.08	0.162±0.007	0.21±0.002
500^{o}C (3:1)	0.86±0.02	0.68±0.02	3.65±0.08	0.26	0.190±0.006	0.19±0.001
400^{o}C (7:1)	0.86	0.06	1.68±0.04	0.04	0.119±0.009	0.17
500^{o}C (7:1)	0.92±0.02	0.05±0.02	3.12±0.10	0.22	0.190±0.005	0.15

Table B.6 Sample data collection, for glucose gasification with NaOH

Operating temperature and water to biomass ratio	H_2 (mmol/g of cellulose)	CH_4 (mmol/g of cellulose)	CO_2 (mmol/g of cellulose)	$C_2+C_3+C_4$ (mmol/g of cellulose)	Gas product (g/g of cellulose)	Solid product (g/g of cellulose)
400^{o}C (3:1)	1.22±0.05	0.08	2.60±0.07	0.09	0.200±0.005	0.24±0.001
500^{o}C (3:1)	1.40±0.02	1.04	3.65±0.13	0.40	0.201±0.002	0.14
400^{o}C (7:1)	1.53	0.96	1.10±0.05	0.12	0.085±0.002	0.14
500^{o}C (7:1)	2.15±0.02	1.16±0.02	2.76±0.09	0.45	0.196±0.005	0.08

B-2 Results from Cellulose Gasification Data Collection

Table B.7 Sample data collection, for cellulose gasification without catalyst

Operating temperature and water to biomass ratio	H_2 (mmol/g of cellulose)	CH_4 (mmol/g of cellulose)	CO_2 (mmol/g of cellulose)	$C_2+C_3+C_4$ (mmol/g of cellulose)	Gas product (g/g of cellulose)	Solid product (g/g of cellulose)
400°C (3:1)	0.50	0.04	1.52±0.05	0.04	0.089±0.002	0.338±0.002
470°C (3:1)	0.72	0.09	1.83±0.04	0.13	0.093±0.001	0.308±0.001
550°C (3:1)	0.95	0.78±0.02	2.26±0.09	0.20	0.120±0.001	0.215±0.002
400°C (7:1)	0.72±0.02	0.06	2.19±0.10	0.03	0.108±0.001	0.277±0.003
470°C (7:1)	0.80	0.33	2.53±0.07	0.04	0.152±0.002	0.246±0.002
550°C (7:1)	1.16±0.04	0.82±0.03	2.88±0.05	0.19	0.164±0.001	0.169±0.002

Table B.8 Sample data collection, for cellulose gasification with calcined dolomite

Operating temperature and water to biomass ratio	H_2 (mmol/g of cellulose)	CH_4 (mmol/g of cellulose)	CO_2 (mmol/g of cellulose)	$C_2+C_3+C_4$ (mmol/g of cellulose)	Gas product (g/g of cellulose)	Solid product (g/g of cellulose)
400^{o}C (3:1)	0.89	0.04	1.85±0.02	0.04	0.149±0.005	0.553±0.03
470^{o}C (3:1)	0.916±0.02	0.06	1.18±0.04	0.07	0.091±0.002	0.492±0.02
550^{o}C (3:1)	1.47±0.02	0.65±0.02	1.60±0.03	0.23	0.052±0.002	0.446±0.02
400^{o}C (7:1)	1.13±0.02	0.18	1.89±0.03	0.11	0.147±0.004	0.506±0.02
470^{o}C (7:1)	1.39±0.01	0.42	1.31±0.03	0.20	0.083±0.002	0.446±0.01
550^{o}C (7:1)	1.69±0.03	0.86±0.02	1.35±0.05	0.29±0.01	0.095±0.001	0.315±0.01

Table B.9 Sample data collection, for cellulose gasification with $Ni/CeO_2/Al_2O_3$

Operating temperature and water to biomass ratio	H_2 (mmol/g of cellulose)	CH_4 (mmol/g of cellulose)	CO_2 (mmol/g of cellulose)	$C_2+C_3+C_4$ (mmol/g of cellulose)	Gas product (g/g of cellulose)	Solid product (g/g of cellulose)
400°C (3:1)	0.91±0.02	0.04	2.49±0.05	0.03	0.102±0.002	0.185±0.002
470°C (3:1)	1.10	0.29	3.82±0.11	0.10	0.187±0.005	0.154±0.003
550°C (3:1)	1.25±0.03	0.86±0.02	4.06±0.12	0.20	0.209±0.005	0.138±0.002
400°C (7:1)	1.07±0.01	0.17	3.50±0.09	0.08	0.178±0.006	0.169±0.003
470°C (7:1)	1.25±0.01	0.44	4.29±0.11	0.17	0.210±0.003	0.138±0.002
550°C (7:1)	1.63±0.05	1.35±0.03	4.68±0.04	0.23	0.244±0.006	0.123±0.004

Table B.10 Sample data collection, for cellulose gasification with KOH

Operating temperature and water to biomass ratio	H_2 (mmol/g of cellulose)	CH_4 (mmol/g of cellulose)	CO_2 (mmol/g of cellulose)	$C_2+C_3+C_4$ (mmol/g of cellulose)	Gas product (g/g of cellulose)	Solid product (g/g of cellulose)
400^{o}C (3:1)	2.05±0.09	0.10	3.04±0.06	0.08	0.296±0.009	0.02
470^{o}C (3:1)	3.08±0.05	0.66±0.01	5.29±0.08	0.24	0.263±0.005	0.02
550^{o}C (3:1)	4.11±0.12	1.84±0.02	7.65±0.12	0.78±0.02	0.403±0.011	0.01
400^{o}C (7:1)	4.48±0.11	0.18	3.12±0.08	0.08	0.190±0.006	0.02
470^{o}C (7:1)	8.03±0.21	1.62±0.01	6.33±0.07	0.36±0.01	0.341±0.008	0.01
550^{o}C (7:1)	9.09±0.06	0.65	6.38±0.05	0.22	0.384±0.012	0.01